Some phenomenological aspects of the 3-3-1 model with the Cárcamo-Kovalenko-Schmidt mechanism

H. N. Long,[1,2,*] N. V. Hop,[3,†] L. T. Hue,[4,5,‡] N. H. Thao,[6,§] and A. E. Cárcamo Hernández[7,‖]

[1]*Theoretical Particle Physics and Cosmology Research Group, Advanced Institute of Materials Science, Ton Duc Thang University, Ho Chi Minh City 700000, Vietnam*

[2]*Faculty of Applied Sciences, Ton Duc Thang University, Ho Chi Minh City 700000, Vietnam*

[3]*Department of Physics, Can Tho University, 3/2 Street, Can Tho 900000, Vietnam*

[4]*Institute for Research and Development, Duy Tan University, Da Nang City 550000, Vietnam*

[5]*Institute of Physics, Vietnam Academy of Science and Technology, 10 Dao Tan, Ba Dinh, Hanoi 100000, Vietnam*

[6]*Department of Physics, Hanoi Pedagogical University 2, Phuc Yen, Vinh Phuc 280000, Vietnam*

[7]*Universidad Técnica Federico Santa María and Centro Científico-Tecnológico de Valparaíso, Casilla 110-V, Valparaíso, Chile*

(Received 18 April 2019; published 8 July 2019)

We perform a comprehensive analysis of several phenomenological aspects of the renormalizable extension of the inert 3-3-1 model with sequentially loop-generated Standard Model fermion mass hierarchy. Special attention is paid to the study of the constraints arising from the experimental data on the ρ parameter, as well as those ones resulting from the charged lepton flavor violating process $\mu \to e\gamma$ and dark matter. We also study the single Z' production via Drell-Yan mechanism at the LHC. We have found that Z' gauge bosons heavier than about 4 TeV comply with the experimental constraints on the oblique ρ parameter as well as with the collider constraints. In addition, we have found that the constraint on the charged lepton flavor violating decay $\mu \to e\gamma$ sets the sterile neutrino masses to be lighter than about 1.12 TeV. In addition the model allows charged lepton flavor violating processes within reach of the forthcoming experiments. The scalar potential and the gauge sector of the model are analyzed and discussed in detail. Our model successfully accommodates the observed dark matter relic density.

DOI: 10.1103/PhysRevD.100.015004

I. INTRODUCTION

Despite its great successes, the Standard Model (SM) does not explain the observed mass and mixing hierarchies in the fermion sector, which remain without a compelling explanation. It is known that in the SM, the masses of the matter fields are generated from the Yukawa interactions. In addition, the Cabibbo–Kobayashi–Maskawa quark mixing matrix is also constructed from the same Yukawa couplings. To solve these puzzles, some mechanisms have been proposed. To the best of our knowledge, the first attempt to explain the huge differences in the SM fermion masses is the Froggatt-Nielsen (FN) mechanism [1]. According to the FM mechanism, the mass differences between generations of fermions arise from suppression factors depending on the FN charges of the particles. It has been noticed that in order to implement the aforementioned mechanism, the effective Yukawa interactions have to be introduced, thus making this theory nonrenormalizable. From this point of view, the recent mechanism proposed by Cárcamo, Kovalenko, and Schmidt [2] (called by CKS mechanism) based on sequential loop suppression mechanism, is more natural since its suppression factor arises from the loop factor $l \approx (1/4\pi)^2$.

One of the main purposes of the models based on the gauge group $SU(3)_C \times SU(3)_L \times U(1)_X$ (for short, 3-3-1 model) [3–10] is concerned with the search of an explanation for the number of generations of fermions. Combined with the QCD asymptotic freedom, the 3-3-1 models provide an explanation for the number of fermion generations. These models have nonuniversal $U(1)_X$ gauge assignments for the left handed quarks fields, thus implying that the cancellation of chiral anomalies is fulfilled when the number of $SU(3)_L$ fermionic triplets is equal to the number of $SU(3)_L$ fermionic antitriplets, which happens

*hoangngoclong@tdtu.edu.vn
†nvhop@ctu.edu.vn
‡lthue@iop.vast.vn
§abcthao@gmail.com
‖antonio.carcamo@usm.cl

when the number of fermion families is a multiple of three. Some other advantages of the 3-3-1 models are: (i) they solve the electric charge quantization [11,12], (ii) they contain several sources of CP violation [13,14], and (iii) they have a natural Peccei-Quinn symmetry, which solves the strong-CP problem [15–18].

In the framework of the 3-3-1 models, most of the research is focused on radiative seesaw mechanisms, and but some involving *nonrenormalizable* interactions introduced to explain the SM fermion mass and mixing pattern (see references in Ref. [19]).

The FN mechanism was implemented in the 3-3-1 models in Ref. [20]. It is interesting to note that the FN mechanism does not produce a new scale since the scale of the flavor breaking is the same as the symmetry breaking scale of the model.

The CKS mechanism has been implemented for the first time in the 3-3-1 model without exotic electric charges ($\beta = -1/\sqrt{3}$) in Ref. [19]. The implementation of the CKS mechanism in the 3-3-1 model leads to viable renormalizable 3-3-1 model that provides a dynamical explanation for the observed SM fermion mass spectrum and mixing parameters consistent with the SM low energy fermion flavor data [19]. It is worth mentioning that the extension of the inert 331 model of Ref. [19] contains a residual discrete $Z_2^{(L_g)}$ lepton number symmetry arising from the spontaneous breaking of the global $U(1)_{L_g}$ symmetry. Under this residual symmetry, the leptons are charged and the other particles are neutral [19].

However, in the mentioned work, the authors have just focused on the data concerning fermions (both quarks and leptons including neutrino mass and mixing), but some questions are open for the future study.

The purpose of this work is to study several phenomenological aspects of the renormalizable extension of the inert 3-3-1 model with sequentially loop-generated SM fermion mass hierarchy. In particular, the constraints arising from the experimental data on the ρ parameter, as well as those ones resulting from the charged lepton flavor violating process $\mu \to e\gamma$ and dark matter. Furthermore our work discusses the Z' production at proton-proton collider via quark-antiquark annihilation. To determine the oblique ρ parameter constraints on the $SU(3)_L \times U(1)_X$ symmetry breaking scale v_χ, which will be used to constrain the heavy Z' gauge boson mass, we proceed to study in detail the gauge and Higgs sectors of the model. In addition we determine the constraints imposed by the charged lepton flavor violating process $\mu \to e\gamma$ and dark matter on the model parameter space. In what regards the scalar potential of the model, due to the implemented symmetries, the Higgs sector is rather simple and can be completely solved. All Goldstone bosons and the SM like Higgs boson are defined.

The further content of this paper is as follows. In Sec. II, we briefly present particle content and SSB of the model. Section III is devoted to gauge boson mass and mixing. Taking into account of data on the ρ parameter, and if only contributions of the gauge bosons are mentioned, we will show that the mass of the heavy neutral boson Z' will be constrained nearly to the excluded regions derived from other experimental data such as LHC searches, and K, D, and B meson mixing. The Higgs sector is considered in Sec. IV. The Higgs sector consists of two parts: the first part contains lepton number conserving terms and the second one is lepton number violating. We study in details the first part and show that the Higgs sector has all necessary ingredients. The ρ parameter will be investigated including Higgs contributions. In Sec. V, lepton flavor violating decays of the charged leptons are discussed, where sterile neutral lepton masses are constrained. Section VI is devoted to the production of the heavy Z' and the heavy neutral scalar H_4. In Sec. VII, we deal with the DM relic density. We make conclusions in Sec. VIII. The scalar potential of the model is given in Appendix.

II. REVIEW OF THE MODEL

To implement the CKS mechanism, only the heaviest particles such as the exotic fermions and the top quark get masses at tree level. The next—medium ones: bottom, charm quarks, tau, and muon get masses at one-loop level. Finally, the lightest particles: up, down, strange quarks and the electron acquire masses at two-loop level. To forbid the usual Yukawa interactions, the discrete symmetries should be implemented. Hence, the full symmetry of the model under consideration is

$$SU(3)_C \times SU(3)_L \times U(1)_X \times Z_4 \times Z_2 \times U(1)_{L_g}, \quad (1)$$

where L_g is the generalized lepton number defined in Refs. [19,21]. It is interesting to note that, in this model, the light active neutrinos get their masses from a combination of linear and inverse seesaw mechanisms at two-loop level.

As in the ordinary 3-3-1 model without exotic electric charges, the quark sector contains the following $SU(3)_C \times SU(3)_L \times U(1)_X$ representations [19]

$$\begin{aligned}
&Q_{nL} = (D_n, -U_n, J_n)_L^T \sim (3, 3^*, 0),\\
&Q_{3L} = (U_3, D_3, T)_L^T \sim \left(3, 3, \frac{1}{3}\right), \qquad n = 1, 2,\\
&D_{iR} \sim \left(3, 1, -\frac{1}{3}\right), \qquad U_{iR} \sim \left(3, 1, \frac{2}{3}\right), \qquad i = 1, 2, 3,\\
&J_{nR} \sim \left(3, 1, -\frac{1}{3}\right), \qquad T_R \sim \left(3, 1, \frac{2}{3}\right),\\
&\tilde{T}_{L,R} \sim \left(3, 1, \frac{2}{3}\right), \qquad B_{L,R} \sim \left(3, 1, -\frac{1}{3}\right), \qquad (2)
\end{aligned}$$

where $\sim$ denotes the quantum numbers for the three above subgroups, respectively. Note that the $SU(3)_L$ singlet exotic up type quarks $\tilde{T}_{L,R}$, down type quarks $B_{L,R}$ in the last line of Eq. (2) are added to the quark spectrum of the ordinary 3-3-1 model in order to implement the CKS mechanism.

In the leptonic sector, besides the usual $SU(3)_L$ lepton triplets, the model contains extra three charged leptons $E_{j(L,R)}$ ($j = 1, 2, 3$) and four neutral leptons, i.e., N_{jR} and Ψ_R ($j = 1, 2, 3$). The leptonic fields have the following $SU(3)_C \times SU(3)_L \times U(1)_X$ assignments:

$$L_{iL} = (\nu_i, e_i, \nu_i^c)_L^T \sim \left(1, 3, -\frac{1}{3}\right), \qquad e_{iR} \sim (1, 1, -1), \quad i = 1, 2, 3, \tag{3}$$

$$\begin{aligned} &E_{1L} \sim (1, 1, -1), \qquad E_{2L} \sim (1, 1, -1), \qquad E_{3L} \sim (1, 1, -1), \\ &E_{1R} \sim (1, 1, -1), \qquad E_{2R} \sim (1, 1, -1), \qquad E_{3R} \sim (1, 1, -1), \\ &N_{1R} \sim (1, 1, 0), \qquad N_{2R} \sim (1, 1, 0), \qquad N_{3R} \sim (1, 1, 0), \qquad \Psi_R \sim (1, 1, 0), \end{aligned} \tag{4}$$

where $\nu_{iL}, \nu^c \equiv \nu_R^c$ and e_{iL} (e_L, μ_L, τ_L) are the neutral and charged lepton families, respectively.

The Higgs sector contains three scalar triplets: χ, η, and ρ and seven singlets φ_1^0, φ_2^0, ξ^0, ϕ_1^+, ϕ_2^+, ϕ_3^+, and ϕ_4^+. Hence, the scalar spectrum of the model is composed of the following fields

$$\chi = \langle\chi\rangle + \chi' \sim \left(1, 3, -\frac{1}{3}\right), \tag{5}$$

$$\begin{aligned} &\langle\chi\rangle = \left(0, 0, \frac{v_\chi}{\sqrt{2}}\right)^T, \qquad \chi' = \left(\chi_1^0, \chi_2^-, \frac{1}{\sqrt{2}}(R_{\chi_3^0} - iI_{\chi_3^0})\right)^T, \\ &\rho = \left(\rho_1^+, \frac{1}{\sqrt{2}}(R_\rho - iI_\rho), \rho_3^+\right)^T \sim \left(1, 3, \frac{2}{3}\right), \\ &\eta = \langle\eta\rangle + \eta' \sim \left(1, 3, -\frac{1}{3}\right), \\ &\langle\eta\rangle = \left(\frac{v_\eta}{\sqrt{2}}, 0, 0\right)^T, \qquad \eta' = \left(\frac{1}{\sqrt{2}}(R_{\eta_1^0} - iI_{\eta_1^0}), \eta_2^-, \eta_3^0\right)^T, \\ &\varphi_1^0 \sim (1, 1, 0), \qquad \varphi_2^0 \sim (1, 1, 0), \\ &\phi_1^+ \sim (1, 1, 1), \qquad \phi_2^+ \sim (1, 1, 1), \qquad \phi_3^+ \sim (1, 1, 1), \qquad \phi_4^+ \sim (1, 1, 1), \\ &\xi^0 = \langle\xi^0\rangle + \xi^{0\prime}, \qquad \langle\xi^0\rangle = \frac{v_\xi}{\sqrt{2}}, \qquad \xi^{0\prime} = \frac{1}{\sqrt{2}}(R_{\xi^0} - iI_{\xi^0}) \sim (1, 1, 0). \end{aligned} \tag{6}$$

The $Z_4 \times Z_2$ assignments of scalar the fields are shown in Table I.

The fields with nonzero lepton number are presented in Table II. Note that the three gauge singlet neutral leptons N_{iR} as well as the elements in the third component of the lepton triplets, namely ν_{iL}^c have lepton number equal -1.

In the model under consideration, the spontaneous symmetry breaking (SSB) occurs by two steps [19]. The first step is triggered by the vacuum expectation values (VEVs) of the χ_3^0 and ξ^0 scalar fields. At this step, all new extra fermions, non-SM gauge bosons, as well as the electrically neutral gauge singlet lepton Ψ_R gain masses. In addition, the entries of the neutral lepton mass matrices with negative lepton number (-1) also get values proportional to v_ξ. At this step, the initial group breaks down to the direct product of the SM gauge group and the $Z_4 \times Z_2^{(L_g)}$ discrete group. The second step is triggered by v_η providing masses for the top quark as well as for the W and Z gauge bosons and leaving the $SU(3)_C \times U(1)_Q \times Z_4 \times Z_2^{(L_g)}$ symmetry preserved. Here $Z_2^{(L_g)}$ is residual symmetry where only leptons are charged, thus forbidding interactions having an odd number of leptons. This is crucial to guarantee the proton stability [19]. Thus

TABLE I. Scalar assignments under $Z_4 \times Z_2$.

	χ	η	ρ	φ_1^0	φ_2^0	ϕ_1^+	ϕ_2^+	ϕ_3^+	ϕ_4^+	ξ^0
Z_4	1	1	-1	-1	i	i	-1	-1	1	1
Z_2	-1	-1	1	1	1	1	1	-1	-1	1

TABLE II. Nonzero lepton number L of fields.

	$T_{L,R}$	$J_{1L,R}$	$J_{2L,R}$	ν^c_{iL}	$e_{iL,R}$	$E_{iL,R}$	N_{iR}	Ψ_R	χ_1^0	χ_2^+	η_3^0	ρ_3^+	ϕ_2^+	ϕ_3^+	ϕ_4^+	ξ^0	$i=1,2,3$
L	-2	2	2	-1	1	1	-1	1	2	2	-2	-2	-2	-2	-2	-2	

$$SU(3)_C \times SU(3)_L \times U(1)_X \times Z_4 \times Z_2 \times U(1)_{L_g} \xrightarrow{v_\chi, v_\xi} SU(3)_C \times SU(2)_L \times U(1)_Y \times Z_4 \times Z_2^{(L_g)} \xrightarrow{v_\eta} SU(3)_C \times U(1)_Q \times Z_4 \times Z_2^{(L_g)}. \quad (7)$$

A consequence of the chain in (7) is

$$v_\eta = v = 246\ \text{GeV} \ll v_\chi \sim v_\xi \sim \mathcal{O}(10)\ \text{TeV}. \quad (8)$$

The corresponding Majoron associated to the spontaneous breaking of the $U(1)_{L_g}$ global symmetry is a gauge-singlet scalar and, therefore, unobservable.

An explanation for the relation $v_\chi \sim v_\xi \sim \mathcal{O}(10)$ TeV is provided in the following. The present lower limits on the Z' gauge boson mass in 3-3-1 models arising from LHC searches reach around 2.5 TeV [22]. These bounds can be translated into limits of about 6.3 TeV on the $SU(3)_C \times SU(3)_L \times U(1)_X$ gauge symmetry breaking scale v_χ. Furthermore, electroweak data from the decays $B_{s,d} \to \mu^+\mu^-$ and $B_d \to K^*(K)\mu^+\mu^-$ set lower bounds on the Z' gauge boson mass ranging from 1 TeV up to 3 TeV [23–27]. Furthermore, as shown in Ref. [28], the experimental data on K, D, and B meson mixings set a lower bound of about 4 TeV for the Z' gauge boson mass in 3-3-1 models, which translates in a lower limit of about 10 TeV for the $SU(3)_L \times U(1)_X$ gauge symmetry breaking scale v_χ.

Finally, to close this section we provide a justification of the role of the different particles of our model:

(1) The presence of the $SU(3)_L$ scalar singlet ϕ_3^+, is needed to generate two loop level down and strange quark masses, as shown in Ref. [19]. Besides that, in order to implement a two loop level radiative seesaw mechanism for the generation of the up, down, and strange quark masses as well as the electron mass, the Z_4 charged $SU(3)_L$ scalar singlets φ_1^0, φ_2^0, ϕ_1^+, ϕ_2^+ (which do not acquire a vacuum expectation value) are also required in the scalar sector. The Z_4 charged $SU(3)_L$ scalar singlet φ_1^0 is also needed to generate one loop level masses for the charm and bottom quarks as well as for the tau and muon leptons. The Z_4 charged $SU(3)_L$ scalar singlets φ_2^0 and ϕ_3^+ as well as the $SU(3)_L$ scalar singlet ϕ_4^+, neutral under Z_4 are also crucial for the implementation of two loop level linear and inverse seesaw mechanisms that give rise to the light active neutrino masses. The $SU(3)_L$ scalar singlet ξ^0 is introduced to spontaneously break the $U(1)_{L_g}$ generalized lepton number symmetry and thus giving rise to a tree-level mass for the right handed Majorana neutrino Ψ_R. It is crucial for generating two loop-level masses for the down and strange quarks.

(2) The $SU(3)_L$ singlet exotic down type quark, i.e., B, is crucial for the implementation of the one loop level radiative seesaw mechanism that generate the bottom quark mass. The $SU(3)_L$ singlet exotic up type quarks, i.e., $\tilde{T}_1$ and $\tilde{T}_2$, are needed to generate a one loop level charm quark mass as well as two loop level down and strange quark masses. The three $SU(3)_L$ singlet exotic charged leptons, i.e., E_j ($j = 1, 2, 3$), are required in order to provide the radiative seesaw mechanisms that generate one loop level tau and muon masses and two loop level electron mass. The four right handed Majorana neutrinos, i.e., N_{jR} ($j = 1, 2, 3$), Ψ_R, are crucial for the implementation of the two loop level linear and inverse seesaw mechanisms that give rise to the light active neutrino masses.

III. GAUGE BOSONS

A. Gauge boson masses and mixing

After SSB, the gauge bosons get masses arising from the kinetic terms for the η and χ $SU(3)_L$ scalar triplets, as follows:

$$L_{\text{mass}}^{\text{gauge}} = (D_\mu \langle\chi\rangle)^\dagger D^\mu \langle\chi\rangle + (D_\mu \langle\eta\rangle)^\dagger D^\mu \langle\eta\rangle, \quad (9)$$

with the covariant derivative for triplet defined as

$$D_\mu = \partial_\mu - igA_{\mu a}\frac{\lambda_a}{2} - ig_X X \frac{\lambda_9}{2} B_\mu, \quad (10)$$

where g and g_X are the gauge coupling constants of the $SU(3)_L$ and $U(1)_X$ groups, respectively. Here, $\lambda_9 = \sqrt{2/3}\,\text{diag}(1,1,1)$ is defined such that $\text{Tr}(\lambda_9\lambda_9) = 2$, similarly as the usual Gell-Mann matrix λ_a, $a = 1, 2, 3, \ldots, 8$. By matching gauge the coupling constants at the $SU(3)_L \times U(1)_X$ symmetry breaking scale, the following relation is obtained [9]

$$t \equiv \frac{g_X}{g} = \frac{3\sqrt{2}\sin\theta_W(M_{Z'})}{\sqrt{3 - 4\sin^2\theta_W(M_{Z'})}}. \quad (11)$$

Let us provide the definition of the Weinberg angle θ_W. As in the SM, one puts $g' = g\tan\theta_W$, where g' is gauge coupling of the $U(1)_Y$ subgroup satisfying the relation [9]

$$g' = \frac{\sqrt{3} g g_X}{\sqrt{18 g^2 - g_X^2}}. \tag{12}$$

Thus

$$\tan\theta_W = \frac{\sqrt{3} g_X}{\sqrt{18 g^2 - g_X^2}}. \tag{13}$$

Denoting

$$W_\mu^\pm = \frac{1}{\sqrt{2}}(A_{\mu 1} \mp i A_{\mu 2}), \qquad Y_\mu^\pm = \frac{1}{\sqrt{2}}(A_{\mu 6} \pm i A_{\mu 7}),$$
$$X_\mu^0 = \frac{1}{\sqrt{2}}(A_{\mu 4} - i A_{\mu 5}), \tag{14}$$

and substituting (10) and (14) into (9) one gets the following squared masses for the charged/non-Hermitian gauge bosons

$$m_W^2 = \frac{g^2}{4} v_\eta^2, \qquad M_{X^0}^2 = \frac{g^2}{4}(v_\chi^2 + v_\eta^2), \qquad M_Y^2 = \frac{g^2}{4} v_\chi^2, \tag{15}$$

where $v_\eta = v = 246$ GeV, as expected.

From Eq. (15) we find the following gauge boson mass squared splitting

$$M_{X^0}^2 - M_Y^2 = m_W^2. \tag{16}$$

For neutral gauge bosons, the squared mass mixing matrix has the form

$$L_{\text{mass}}^{\text{ngauge}} = \frac{1}{2} V^T M_{\text{ngauge}}^2 V, \tag{17}$$

where $V^T = (A_{\mu 3}, A_{\mu 8}, B_\mu)$ and

$$M_{\text{ngauge}}^2 = \frac{g^2}{4}\begin{pmatrix} v_\eta^2 & \frac{v_\eta^2}{\sqrt{3}} & -\frac{2t}{3\sqrt{6}} v_\eta^2 \\ & \frac{1}{3}(4v_\chi^2 + v_\eta^2) & \frac{2t}{9\sqrt{2}}(2v_\chi^2 - v_\eta^2) \\ & & \frac{2t^2}{27}(v_\chi^2 + v_\eta^2) \end{pmatrix}. \tag{18}$$

The down-left entries in (18) are not written, due to the fact that the above matrix is symmetric.

The matrix in (18) has vanishing determinant, thus giving rise to a massless gauge boson, which corresponds to the photon. The diagonalization of the squared mass matrix for neutral gauge bosons of Eq. (18) is divided in two steps. In the first step, the massive fields are identified as

$$A_\mu = s_W A_{\mu 3} + c_W\left(-\frac{t_W}{\sqrt{3}} A_{\mu 8} + \sqrt{1 - \frac{t_W^2}{3}} B_\mu\right),$$
$$Z_\mu = c_W A_{\mu 3} - s_W\left(-\frac{t_W}{\sqrt{3}} A_{\mu 8} + \sqrt{1 - \frac{t_W^2}{3}} B_\mu\right),$$
$$Z'_\mu = \sqrt{1 - \frac{t_W^2}{3}} A_{\mu 8} + \frac{t_W}{\sqrt{3}} B_\mu, \tag{19}$$

where we have denoted $s_W = \sin\theta_W$, $c_W = \cos\theta_W$, $t_W = \tan\theta_W$. The coupling of the photon A_μ gives $e = g s_W$. After the first step, the squared mass matrix is a block diagonal one in the new basis (A_μ, Z_μ, Z'_μ), where the entry in the top is zero (due to the masslessness of the photon), while the 2×2 matrix for (Z_μ, Z'_μ) in the bottom has the form

$$M_{(2\times 2)}^2 = \begin{pmatrix} M_Z^2 & M_{ZZ'}^2 \\ M_{ZZ'}^2 & M_{Z'}^2 \end{pmatrix}. \tag{20}$$

The matrix elements in (20) are given by

$$M_Z^2 = \frac{g^2 v_\eta^2}{4 c_W^2} = \frac{m_W^2}{c_W^2},$$
$$M_{ZZ'}^2 = \frac{g^2}{4 c_W^2 \sqrt{3 - 4 s_W^2}} v_\eta^2 (1 - 2 s_W^2),$$
$$M_{Z'}^2 = \frac{g^2 c_W^2}{4(3 - 4 s_W^2)}\left[4 v_\chi^2 + \frac{v_\eta^2 (1 - 2 s_W^2)^2}{c_W^4}\right]. \tag{21}$$

Note that our formula of $M_{Z'}^2$ is consistent with that given in [23].

In the last step of diagonalization, the $Z - Z'$ mixing angle ϕ and mass eigenstates $Z^{1,2}$ are determined as

$$\tan 2\phi = \frac{2 M_{ZZ'}^2}{M_{Z'}^2 - M_Z^2}, \tag{22}$$

$$Z_\mu^1 = Z_\mu \cos\phi - Z'_\mu \sin\phi,$$
$$Z_\mu^2 = Z_\mu \sin\phi + Z'_\mu \cos\phi. \tag{23}$$

Our definition of ϕ is consistent with that in Ref. [29] needed to study the ρ parameter.

The masses of physical neutral gauge bosons are determined as

$$M_{Z^1}^2 = \frac{1}{2}\{M_{Z'}^2 + M_Z^2 - [(M_{Z'}^2 - M_Z^2)^2 + 4(M_{ZZ'}^2)^2]^{\frac{1}{2}}\},$$
$$M_{Z^2}^2 = \frac{1}{2}\{M_{Z'}^2 + M_Z^2 + [(M_{Z'}^2 - M_Z^2)^2 + 4(M_{ZZ'}^2)^2]^{\frac{1}{2}}\}. \tag{24}$$

In the limit $v_\chi^2 \gg v_\eta^2$, one approximates

$$M_{Z^1}^2 \simeq M_Z^2 - \frac{(M_{ZZ'}^2)^2}{M_{Z'}^2} + M_Z^2 \times \mathcal{O}\left(\frac{v_\eta^4}{v_\chi^4}\right), \tag{25}$$

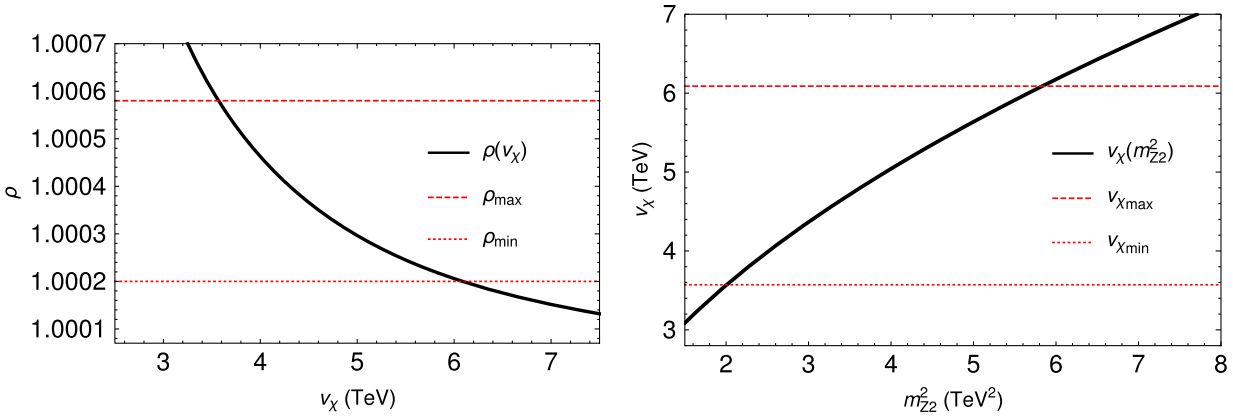

FIG. 1. Left-panel: ρ parameter as a function of v_χ, upper and lower horizontal lines are upper and lower limits in (31). Right-panel: Relation between v_χ and $M^2_{Z_2}$, upper horizontal lines are an upper and a lower limits of v_χ, respectively.

$$M^2_{Z^2} \simeq M^2_{Z'} + \frac{(M^2_{ZZ'})^2}{M^2_{Z'}} + M^2_Z \times \mathcal{O}\left(\frac{v^4_\eta}{v^4_\chi}\right) \simeq M^2_{Z'}. \quad (26)$$

$$\tan\phi \simeq \frac{(1-2s^2_W)\sqrt{3-4s^2_W}}{4c^4_W}\left(\frac{v^2_\eta}{v^2_\chi}\right). \quad (27)$$

B. Limit on Z' mass from the ρ parameter

The presence of the non-SM particles modifies the oblique corrections of the SM, the values of which have been extracted from high precision experiments. Consequently, the validity of our model depends on the condition that the non-SM particles do not contradict those experimental results. Let us note that one of the most important observables in the SM is the ρ parameter defined as

$$\rho = \frac{m^2_W}{c^2_W M^2_Z}. \quad (28)$$

For the model under consideration, one-loop contributions of the new heavy gauge bosons to the oblique correction lead to the following form of the ρ parameter [29]

$$\rho - 1 \simeq \tan^2\phi\left(\frac{M^2_{Z'}}{m^2_Z} - 1\right) + \frac{3\sqrt{2}G_F}{16\pi^2}\left[M^2_+ + M^2_0 + \frac{2M^2_+M^2_0}{M^2_+ - M^2_0}\ln\frac{M^2_0}{M^2_+}\right] - \frac{\alpha(m_Z)}{4\pi s^2_W}\left[t^2_W \ln\frac{M^2_0}{M^2_+} + \frac{\varepsilon^2(M_+, M_0)}{2} + O(\varepsilon^3(M_+, M_0))\right], \quad (29)$$

where $M_0 = M_{X^0}, M_+ = M_{Y^+}$ and $\varepsilon(M,m) \equiv \frac{M^2-m^2}{m^2}$.

Combining with Eq. (16), one gets

$$\rho - 1 \simeq \tan^2\phi\left(\frac{M^2_{Z'}}{m^2_Z} - 1\right) + \frac{3\sqrt{2}G_F}{16\pi^2}\left[2M^2_{Y^+} + m^2_W - \frac{2M^2_{Y^+}(M^2_{Y^+}+m^2_W)}{m^2_W}\ln\frac{(M^2_{Y^+}+m^2_W)}{M^2_{Y^+}}\right] - \frac{\alpha(m_Z)}{4\pi s^2_W}\left[t^2_W \ln\frac{(M^2_{Y^+}+m^2_W)}{M^2_{Y^+}} + \frac{m^4_W}{2(M^2_{Y^+}+m^2_W)^2}\right], \quad (30)$$

where $\alpha(m_Z) \approx \frac{1}{128}$ [30].

Taking into account $s^2_W = 0.23122$ [30] and

$$\rho = 1.00039 \pm 0.00019, \quad (31)$$

we have plotted $\Delta\rho$ as a function of v_χ in Fig. 1 (the left-panel). From Fig. 1 (the left-panel), it follows

$$3.57\ \text{TeV} \le v_\chi \le 6.09\ \text{TeV}. \quad (32)$$

Substituting (32) into (26) and evaluating in Fig. 1 (the right-panel) we get a bound on the Z' mass as follows

$$1.42\ \text{TeV} \le M_{Z^2} \le 2.42\ \text{TeV}. \quad (33)$$

Then, the bilepton gauge boson mass is constrained to be in the range:

$$465\ \text{GeV} \leq M_Y \leq 960\ \text{GeV}, \tag{34}$$

where $m_W = 80.379$ GeV [30]. The above limit is stronger than the one obtained from the wrong muon decay $M_Y \geq 230$ GeV [31].

It is worth mentioning that the second term in (30) is much smaller the first one. Consequently, the limit derived from the tree level contribution is very close to the one obtained when we consider the radiative corrections arising from heavy vector exchange.

From LHC searches, it follows that the lower bound on the Z' boson mass in 3-3-1 models ranges from 2.5 to 3 TeV [22,32]. From the decays $B_{s,d} \to \mu^+\mu^-$ and $B_d \to K^*(K)\mu^+\mu^-$ [23–27], the lower limit on the Z' boson mass ranges from 1 TeV to 3 TeV. We will show that when scalar contributions to the ρ parameter are included, there will exist allowed m_{Z_2} values larger than the range given in (33), so that they satisfy the recent lower bounds concerned from LHC searches.

For conventional notation, hereafter we will call Z^1 and Z^2 by Z and Z', respectively.

Now we turn to the main subject—the Higgs sector.

IV. ANALYSIS OF THE LEPTON NUMBER CONSERVING PART OF THE SCALAR POTENTIAL

Below we present lepton number conserving part V_{LNC} of the scalar potential of the model shown in Appendix. Expanding the Higgs potential around the VEVs, one gets the scalar potential minimization conditions at tree level as follows

$$w_3 = 0, \tag{35}$$

$$\begin{aligned} -\mu_\chi^2 &= v_\chi^2\lambda_{13} + \frac{1}{2}v_\eta^2\lambda_5 + \frac{1}{2}\lambda_{\chi\xi}v_\xi^2, \\ -\mu_\eta^2 &= v_\eta^2\lambda_{17} + \frac{1}{2}v_\chi^2\lambda_5 + \frac{1}{2}\lambda_{\eta\xi}v_\xi^2, \\ -\mu_\xi^2 &= \frac{1}{2}\lambda_{\chi\xi}v_\chi^2 + \frac{1}{2}\lambda_{\eta\xi}v_\eta^2 + \lambda_\xi v_\xi^2. \end{aligned} \tag{36}$$

From the analysis of the scalar potential, taking into account the constraint conditions of Eq. (35), we find that the charged scalar sector is composed of two massless fields, i.e., η_2^+ and χ_2^+ which are the Goldstone bosons eaten by the longitudinal components of the W^+ and Y^+ gauge bosons, respectively. The other massive electrically charged fields are ϕ_1^+, ϕ_2^+ and ϕ_4^+ whose masses are respectively given by:

$$\begin{aligned} m^2_{\phi_1^+} &= \mu^2_{\phi_1^+} + \frac{1}{2}[v_\chi^2\lambda_1^{\chi\phi} + v_\eta^2\lambda_1^{\eta\phi} + v_\xi^2\lambda_1^{\phi\xi}], \\ m^2_{\phi_2^+} &= \mu^2_{\phi_2^+} + \frac{1}{2}[v_\chi^2\lambda_2^{\chi\phi} + v_\eta^2\lambda_2^{\eta\phi} + v_\xi^2\lambda_2^{\phi\xi}], \\ m^2_{\phi_4^+} &= \mu^2_{\phi_4^+} + \frac{1}{2}[v_\chi^2\lambda_4^{\chi\phi} + v_\eta^2\lambda_4^{\eta\phi} + v_\xi^2\lambda_4^{\phi\xi}]. \end{aligned} \tag{37}$$

In addition, the basis $(\rho_1^+, \rho_3^+, \phi_3^+)$ corresponds to the following squared mass matrix

$$M^2_{\text{charged}} = \begin{pmatrix} A + \frac{1}{2}v_\eta^2(\lambda_6 + \lambda_9) & 0 & \frac{1}{2}v_\eta v_\xi \lambda_3 \\ 0 & A + \frac{1}{2}(v_\chi^2\lambda_7 + v_\eta^2\lambda_6) & \frac{1}{\sqrt{2}}v_\chi w_2 \\ \frac{1}{2}v_\eta v_\xi\lambda_3 & \frac{1}{\sqrt{2}}v_\chi w_2 & \mu^2_{\phi_3^+} + B_3 \end{pmatrix}, \tag{38}$$

where we have used the following notations

$$\begin{aligned} A &\equiv \mu_\rho^2 + \frac{1}{2}[v_\chi^2\lambda_{18} + \lambda_{\rho\xi}v_\xi^2], \\ B_i &\equiv \frac{1}{2}(v_\chi^2\lambda_i^{\chi\phi} + v_\eta^2\lambda_i^{\eta\phi} + v_\xi^2\lambda_i^{\phi\xi}), \quad i = 1,2,3,4. \end{aligned} \tag{39}$$

From (38), it follows that in the limit $v_\eta \ll v_\xi$, ρ_1^+ is a physical field with mass

$$m^2_{\rho_1^+} = A + \frac{1}{2}v_\eta^2(\lambda_6 + \lambda_9), \tag{40}$$

while the two massive *bilepton* scalars ρ_3^+ and ϕ_3^+ mix with each other.

Now we turn into CP-odd Higgs sector. There are three massless fields: $I_{\chi_3^0}, I_{\eta_1^0}$, and I_{ξ^0}. The field I_{φ_2} is a physical state itself with squared mass

$$m^2_{I_{\varphi_2}} = \mu^2_{\varphi_2} + B'_2, \tag{41}$$

where

$$B'_n \equiv \frac{1}{2}(v_\chi^2\lambda_n^{\chi\varphi} + v_\eta^2\lambda_n^{\eta\varphi} + v_\xi^2\lambda_n^{\varphi\xi}), \quad n = 1,2. \tag{42}$$

The squared mass matrix of the four remaining CP-odd Higgs fields separate into two block diagonal submatrices corresponding to the two original base $(I_{\chi_1^0}, I_{\eta_3^0})$ and (I_{φ_1}, I_ρ), namely

$$\begin{aligned} m^2_{CP\text{odd1}} &= \frac{\lambda_8}{2}\begin{pmatrix} v_\eta^2 & -v_\chi v_\eta \\ -v_\chi v_\eta & v_\chi^2 \end{pmatrix}, \\ m^2_{CP\text{odd2}} &= \begin{pmatrix} \mu^2_{\varphi_1} + B'_1 - C & \frac{1}{2}v_\chi v_\eta(\lambda_1 - \lambda_2) \\ \frac{1}{2}v_\chi v_\eta(\lambda_1 - \lambda_2) & A + \frac{\lambda_6}{2}v_\eta^2 \end{pmatrix}, \end{aligned} \tag{43}$$

where

$$C \equiv v_\chi^2\lambda_{22} + v_\eta^2\lambda_{24} + v_\xi^2\lambda_{25} \tag{44}$$

The first matrix in (43) provides two mass eigenstates, where one of them is massless,

$$\begin{aligned} G_1 &= \cos\theta_a I_{\chi_1^0} + \sin\theta_a I_{\eta_3^0}, \qquad m_{G_1} = 0, \\ A_1 &= -\sin\theta_a I_{\chi_1^0} + \cos\theta_a I_{\eta_3^0}, \qquad m_{A_1}^2 = \frac{\lambda_8 v_\chi^2}{2\cos^2\theta_a}, \end{aligned} \tag{45}$$

where

$$\tan\theta_a = \frac{v_\eta}{v_\chi}. \tag{46}$$

The physical states relating to the second matrix in (43) are

$$\begin{pmatrix} A_2 \\ A_3 \end{pmatrix} = \begin{pmatrix} \cos\theta_\rho & \sin\theta_\rho \\ -\sin\theta_\rho & \cos\theta_\rho \end{pmatrix} \begin{pmatrix} I_{\varphi_1} \\ I_\rho \end{pmatrix}, \tag{47}$$

where the mixing angle is given by

$$\tan 2\theta_\rho = \frac{v_\chi v_\eta(\lambda_1 - \lambda_2)}{(\mu_{\varphi_1}^2 - C + B_1' - A - \frac{\lambda_6}{2}v_\eta^2)}. \tag{48}$$

Their squared masses are

$$m_{A_{2,3}}^2 = \frac{1}{2}\left\{A + D_1 \mp \sqrt{(A - D_1)^2 + v_\eta^2[2(A - D_1)\lambda_6 + v_\eta^2\lambda_6^2 + v_\chi^2(\lambda_{13} - \lambda_{14})^2]}\right\}, \tag{49}$$

where $D_1 = \mu_{\varphi_1}^2 + B_1' - C + \frac{1}{2}v_\eta^2\lambda_6$.

Next, the CP-even scalar sector is our task. We find that R_{φ_2} is physical with mass

$$m_{R_{\varphi_2}}^2 = m_{I_{\varphi_2}}^2 = \mu_{\varphi_2}^2 + \frac{1}{2}(v_\chi^2\lambda_2^{\chi\varphi} + v_\eta^2\lambda_2^{\eta\varphi} + v_\xi^2\lambda_2^{\varphi\xi}). \tag{50}$$

As mentioned in Ref. [19], the lightest scalar φ_2^0 is a possible DM candidate with light mass smaller than 1 TeV. Therefore, Eq. (50) suggests a reasonable assumption

$$\mu_{\varphi_2}^2 = -\frac{1}{2}(v_\chi^2\lambda_2^{\chi\varphi} + v_\xi^2\lambda_2^{\varphi\xi}). \tag{51}$$

In this case, the model contains the complex scalar DM φ_2^0 with mass $m_{R_{\varphi_2}}^2 = m_{I_{\varphi_2}}^2 = \frac{1}{2}\lambda_2^{\eta\varphi}v_\eta^2$.

There are other seven CP-even Higgs components which the squared mass matrix separates into two 2×2 and one 3×3 independent matrices. The 2×2 matrices are

$$\begin{aligned} m_{CP\text{even1}}^2 &= \frac{\lambda_8}{2}\begin{pmatrix} v_\eta^2 & v_\chi v_\eta \\ v_\chi v_\eta & v_\chi^2 \end{pmatrix}, \\ m_{CP\text{even2}}^2 &= \begin{pmatrix} A + \frac{\lambda_6}{2}v_\eta^2 & -\frac{1}{2}v_\chi v_\eta(\lambda_1 + \lambda_2) \\ -\frac{1}{2}v_\chi v_\eta(\lambda_1 + \lambda_2) & \mu_{\varphi_1}^2 + C + B_1' \end{pmatrix}, \end{aligned} \tag{52}$$

corresponding to the two original base $(R_{\chi_1^0}, R_{\eta_3^0})$ and (R_ρ, R_{φ_1}), respectively. The physical states of the first matrix in (52) are determined as follows,

$$\begin{aligned} R_{G_1} &= \cos\theta_a R_{\chi_1^0} + \sin\theta_a R_{\eta_3^0}, \qquad m_{R_{G_1}} = 0, \\ H_1 &= -\sin\theta_a R_{\chi_1^0} + \cos\theta_a R_{\eta_3^0}, \quad m_{H_1}^2 = m_{A_1}^2 = \frac{\lambda_8 v_\chi^2}{2\cos^2\theta_a}. \end{aligned} \tag{53}$$

The physical states of the second matrix in (52) are

$$\begin{pmatrix} H_2 \\ H_3 \end{pmatrix} = \begin{pmatrix} \cos\theta_r & \sin\theta_r \\ -\sin\theta_r & \cos\theta_r \end{pmatrix} \begin{pmatrix} R_\rho \\ R_{\varphi_1} \end{pmatrix}, \tag{54}$$

where the mixing angle is

$$\tan 2\theta_r = \frac{v_\chi v_\eta(\lambda_1 + \lambda_2)}{(\mu_{\varphi_1}^2 + C + B_1' - A - \frac{\lambda_6}{2}v_\eta^2)} \tag{55}$$

and their squared masses are

$$m_{H_{2,3}}^2 = \frac{1}{2}\left\{A + D_2 \mp \sqrt{(A - D_2)^2 + v_\eta^2[2(A - D_2)\lambda_6 + v_\eta^2\lambda_6^2 + v_\chi^2(\lambda_{13} + \lambda_{14})^2]}\right\}, \tag{56}$$

where $D_2 = \mu_{\varphi_1}^2 + B_1' + C + \frac{1}{2}v_\eta^2\lambda_6$.

The squared mass matrix corresponding to the basis $(R_{\chi_3^0}, R_{\eta_1^0}, R_{\xi^0})$ is

$$m^2_{CP\text{even}3} = \begin{pmatrix} 2v_\chi^2\lambda_{13} & v_\chi v_\eta \lambda_5 & \lambda_{\chi\xi} v_\chi v_\xi \\ v_\chi v_\eta \lambda_5 & 2v_\eta^2 \lambda_{17} & \lambda_{\eta\xi} v_\eta v_\xi \\ \lambda_{\chi\xi} v_\chi v_\xi & \lambda_{\eta\xi} v_\eta v_\xi & 2\lambda_\xi v_\xi^2 \end{pmatrix}, \quad (57)$$

which contains a SM-like Higgs boson found by LHC. The mass eigenstates will be discussed using simplified conditions.

Let us summarize the Higgs content:

(1) In the charged scalar sector: there are two Goldstone bosons η^- and χ^- eaten by the gauge bosons W^- and Y^-. Three massive charged Higgs bosons are ϕ_1^+, ϕ_2^+, and ϕ_4^+. The remaining fields ρ_1^+, ϕ_3^+, and ρ_3^+ are mixing.

(2) In the CP-odd scalar sector: there is one massless Majoron scalar I_{ξ^0} which is denoted by G_M. Fortunately, it is a gauge singlet, therefore, is *phenomenologically harmless*. Two massless scalars $I_{\eta_1^0}$ and $I_{\chi_3^0}$ are Goldstone bosons for the gauge bosons Z and Z', respectively. There exists another massless state denoted by G_1, its role will be discussed below. Here we just mention that in the limit $v_\eta \ll v_\chi$, this field is $I_{\chi_1^0}$. The massive CP-odd field are I_{φ_2}, A_1 and other two I_{φ_1}, I_ρ are mixing.

(3) In the CP-even scalar sector: There is one massless field: R_{G_2}, and in the limit $v_\eta \ll v_\chi$, it tends to $R_{\chi_1^0}$. Combination of G_1 and R_{G_1} is Goldstone boson for neutral bilepton gauge boson X^0, namely $G_{X^0} = \frac{1}{\sqrt{2}}(R_{G_1} - iG_1)$. The massive fields are R_{φ_2}, H_1, H_2 and three massive R_χ, R_η, R_{ξ^0} and the SM-like Higgs boson h. Note that *there exists degeneracy in Eqs. (50) and (53) when the contribution arising from $Z_2 \times Z_4$ soft breaking scalar interactions is not considered*. Thus, the complex scalar φ_2 has mass given by Eq. (50), which is consistent with the prediction in Ref. [19]. To be a DM candidate, the condition (51) can be used to eliminate the terms with large VEVs such as v_χ and v_ξ. As a result, the mass of the DM candidate is

$$m^2_{\varphi_2} = \frac{1}{2} v_\eta^2 \lambda_2^{\eta\varphi}. \quad (58)$$

According [30], the weakly interacting massive particles (WIMP) candidate has mass around 10 GeV, implying that $\lambda_2^{\eta\varphi} \approx 0.04$. To get the second DM candidate, namely, φ_1^0, we have to carefully choose conditions.

Equations (45) and (53) result in a new complex w defined as follows

$$\omega = \frac{1}{\sqrt{2}}(H_1 - iA_1), \qquad m^2_\omega = \frac{\lambda_8 v_\chi^2}{2\cos^2\theta_a}. \quad (59)$$

Let us rewrite the Higgs content in terms of the mass eigenstates mentioned above:

$$\chi \simeq \begin{pmatrix} G_{X^0} \\ G_{Y^-} \\ \frac{1}{\sqrt{2}}(v_\chi + R_{\chi_3^0} - iG_{Z'}) \end{pmatrix}, \qquad \rho = \begin{pmatrix} \rho_1^+ \\ \frac{1}{\sqrt{2}}(R_\rho - iI_\rho) \\ \rho_3^+ \end{pmatrix}, \qquad \eta \simeq \begin{pmatrix} \frac{1}{\sqrt{2}}(v_\eta + h - iG_Z) \\ G_{W^-} \\ \omega \end{pmatrix},$$
$$\varphi_2^0 = \frac{1}{\sqrt{2}}(R_{\varphi_2} - iI_{\varphi_2}) \sim (1,1,0,i,1,0) \sim \text{DM candidate},$$
$$\xi^0 = \frac{1}{\sqrt{2}}(v_\xi + R_{\xi^0} - iG_M) \sim (1,1,0). \quad (60)$$

A. Simplified solutions

We have shown that the mass eigenstates of scalars have been determined explicitly, except those relating to the two 3×3 matrices (38) and (57). By introducing some further constrained assumptions to simplify these matrices so that the physical states can be found, we will point out that the parameter space of the model under consideration contains valid regions, which are consistent with the experiment data including the ρ parameter. To reduce the arbitrary of the unknown Higgs couplings in the potential (A1), the following relations are assumed first

$$\lambda_1 = \lambda_2, \quad \lambda_{15} = \lambda_{16}, \quad \lambda_{19} = \lambda_{20}, \quad w_1 = w_4. \quad (61)$$

In the next steps, we just pay attention to find the masses and mass eigenstates of the two matrices (38) and (57). The other will be summarized if necessary.

1. The CP-odd Higgs bosons

Under the assumption (61), the CP-odd scalar sector consists of four massless fields $\{I_{\chi_3^0}, I_\eta, G_M, G_1\}$ and four massive fields $\{A_1, A_2, A_3 I_{\varphi_2}\}$, as summarized in Table III.

TABLE III. Squared mass of CP-odd scalars under condition in (61) and $v_\chi \gg v_\eta$.

Fields	$I_{\chi_1^0} = G_1 \in G_{X^0}$	$I_{\chi_3^0} = G_{Z'}$	$I_{\eta_1^0} = G_Z$	$I_{\eta_3^0} = A_1$	$I_\rho = A_2$	$I_{\varphi_1^0} = A_3$	$I_{\varphi_2^0} = DM$	$I_{\xi^0} = G_M$
Squared mass	0	0	0	$m^2_{A_1}$	$m^2_{A_2}$	$m^2_{A_3}$	$m^2_{I_{\varphi_2^0}}$	0

TABLE IV. Squared masses of CP-even scalars under condition in (62) and $v_\chi \gg v_\eta$.

Fields	$R_{\chi_1^0} \in G_{X^0}$	$R_{\chi_3^0} \simeq H_4$	$R_{\eta_1^0} = h$	$R_{\eta_3^0} = H_1$	$R_\rho = H_2$	$R_{\varphi_1^0} = H_3$	$R_{\varphi_2^0} = DM$	$R_{\xi^0} \simeq H_5$
Squared mass	0	λv_χ^2	$\frac{4}{3}\lambda v_\eta^2$	$m^2_{H_1} = m^2_{A_1}$	$m^2_{H_2}$	$m^2_{H_3}$	$m^2_{R_{\varphi_2^0}} = m^2_{I_{\varphi_2^0}}$	$3\lambda v_\chi^2$

2. The CP-even and SM-like Higgs bosons

Now we turn to the sector where the SM Higgs boson exists, i.e., the matrix in the basis $(R_{\chi_3^0}, R_{\eta_1^0}, R_{\xi^0})$ is given by Eq. (57). Let us assume a simplified scenario worth to be considered is characterized by the following relations:

$$\lambda_5 = \lambda_{13} = \lambda_{17} = \lambda_\xi = \lambda_{\chi\xi} = \lambda_{\eta\xi} = \lambda, \qquad v_\xi = v_\chi. \quad (62)$$

In this scenario, the squared matrix (57) takes the simple form:

$$m^2_{CP\text{even3}} = \lambda \begin{pmatrix} 2x^2 & x & x \\ x & 2 & 1 \\ x & 1 & 2 \end{pmatrix} v_\chi^2, \qquad x = \frac{v_\eta}{v_\chi} = \tan\theta_a. \quad (63)$$

Because $v_\chi \gg v_\eta$, the matrix (63) can be perturbatively diagonalized as follows:

$$R^T_{CP\text{even3}} m^2_{CP\text{even3}} R_{CP\text{even3}} \simeq \begin{pmatrix} \frac{4}{3}\lambda v_\eta^2 & 0 & 0 \\ 0 & \lambda v_\chi^2 & 0 \\ 0 & 0 & 3\lambda v_\chi^2 \end{pmatrix},$$

$$R_{CP\text{even3}} \simeq \begin{pmatrix} -1 + \frac{x^2}{9} & 0 & \frac{\sqrt{2}}{3}x \\ \frac{x}{3} & -\sqrt{\frac{1}{2}} & \sqrt{\frac{1}{2}} \\ \frac{x}{3} & \sqrt{\frac{1}{2}} & \sqrt{\frac{1}{2}} \end{pmatrix}, \quad (64)$$

Thus, we find that the physical scalars included in the matrix $m^2_{CP\text{even3}}$ are

$$\begin{pmatrix} h \\ H_4 \\ H_5 \end{pmatrix} \simeq \begin{pmatrix} -1 + \frac{x^2}{9} & \frac{x}{3} & \frac{x}{3} \\ 0 & -\sqrt{\frac{1}{2}} & \sqrt{\frac{1}{2}} \\ \frac{\sqrt{2}}{3}x & \sqrt{\frac{1}{2}} & \sqrt{\frac{1}{2}} \end{pmatrix} \begin{pmatrix} R_{\eta_1^0} \\ R_{\chi_3^0} \\ R_{\xi^0} \end{pmatrix}, \quad (65)$$

where h is the SM-like Higgs boson with mass 126 GeV identified with that found by LHC, whereas H_4 and H_5 are physical heavy scalars acquiring masses at the breaking scale of the $SU(3)_L \times U(1)_X \times Z_4 \times Z_2 \times U(1)_{L_g}$ symmetry. Thus, we find that h has couplings very close to SM expectation with small deviations of the order of $\frac{v_\eta^2}{v_\chi^2} \sim \mathcal{O}(10^{-3})$. In addition, the squared masses of the physical scalars h and $H_{4,5}$ are given in (64).

Now, the content of the CP-even scalar sector is summarized in Table IV.

Taking into account mass of the SM Higgs boson equal 126 GeV, from Table IV we obtain $\lambda \approx 0.187$, which can be used to calculate masses of the $H_{4,5}$ once v_χ is fixed.

3. The charged Higgs bosons

The charged scalar sector contains two massless fields: G_{W^+} and G_{Y^+} which are Goldstone bosons eaten by the longitudinal components of the W^+ and Y^+ gauge bosons, respectively. The other massive fields are ϕ_1^+, ϕ_2^+, and ϕ_4^+ with respective masses given in (39).

In the basis $(\rho_1^+, \rho_3^+, \phi_3^+)$, the squared mass matrix is given in (38). Let us make effort to simplify this matrix. Note that μ_χ^2, μ_η^2, and μ_ξ^2 can be derived using relations (35) and (62). In addition, it is reasonable to assume

$$\mu_\rho^2 = -\frac{v_\chi^2}{2}(\lambda_{18} + \lambda_{\rho\xi}) \approx \mu_\eta^2, \qquad \mu^2_{\phi_3^+} = -\frac{v_\chi^2}{2}(\lambda_2^{\chi\phi} + \lambda_2^{\phi\xi}), \quad (66)$$

we obtain the simple form of the squared mass matrix of the charged Higgs bosons,

$$M^2_{\text{chargeds}} = \begin{pmatrix} \frac{1}{2}v_\eta^2(\lambda_6 + \lambda_9) & 0 & \frac{\lambda_3}{2}v_\eta v_\chi \\ 0 & \frac{1}{2}(v_\chi^2\lambda_7 + \lambda_6 v_\eta^2) & \frac{1}{\sqrt{2}}v_\chi w_2 \\ \frac{\lambda_3}{2}v_\eta v_\chi & \frac{1}{\sqrt{2}}v_\chi w_2 & \frac{1}{2}v_\eta^2\lambda_2^{\eta\phi} \end{pmatrix}. \quad (67)$$

The matrix (67) predicts that there may exist two light charged Higgs bosons $H^+_{1,2}$ with masses at the electroweak

TABLE V. Squared mass of charged scalars under condition in (66) and $v_\chi \gg v_\eta$.

Fields	$\eta_2^+ = G_{W^+}$	$\chi_2^+ = G_{Y^+}$	H_1^+	H_3^+	H_2^+	ϕ_1^+	ϕ_2^+	ϕ_4^+
Squared mass	0	0	$m^2_{H_1^+}$	$m^2_{H_3^+}$	$m^2_{H_2^+}$	$m^2_{\phi_1^+}$	$m^2_{\phi_2^+}$	$m^2_{\phi_4^+}$

scale and the mass of H_3^+ which is mainly composed of ρ_3^+ is around 3.5 TeV. In addition, the Higgs boson H_1^+ almost does not carry lepton number, whereas the others two do.

Generally, the Higgs potential always contains mass terms which mix VEVs. However, these terms must be small enough to avoid high order divergences (for examples, see Refs. [33,34]) and provide baryon asymmetry of Universe by the strong electroweak phase transition (EWPT).

Ignoring the mixing term containing λ_3 in (67) does not affect other physical aspects, since the above-mentioned term just increases or decreases a small amount of the charged Higgs bosons. Therefore, without loss of generality, neglecting the term with λ_3 satisfies other aims such as EWPT.

Hence, in the matrix of (67), the coefficient λ_3 is reasonably assumed to be zero. Therefore we get immediately one physical field ρ_1^+ with mass given by

$$m^2_{\rho_1^+} = \frac{1}{2} v_\eta^2 (\lambda_6 + \lambda_9). \tag{68}$$

The other fields mix by submatrix given at the bottom of (67). The limit $\rho_1^+ = H_1^+$ when $\lambda_3 = 0$ is very interesting for discussion of the Higgs contribution to the ρ parameter.

The content of the charged scalar sector is summarized in Table V. It is worth mentioning that the masses of three charged scalars ϕ_i^+, $i = 1, 2, 4$ are still not fixed.

The potential including lepton number violations, i.e., $V_{\text{full}} = V_{\text{LNC}} + V_{\text{LNV}}$ is quite similar to the previous one. There are some differences:

(1) The masses of the fields receive some new contributions.
(2) The complex scalar φ_2^0 has the same mass in both cases.
(3) Majoron does not exist and its mass only arises from lepton number violating scalar interactions.
(4) The mixing of the CP-even scalar fields is more complicated.

B. Scalar contributions to the ρ parameter

The new Higgs bosons may give contribution to the ρ parameter at one-loop level, as shown in many models beyond the SM, such as the simplified models [35], the two Higgs doublet models [36,37], and the supersymmetric version of the SM [38]. In the 3-3-1 CKS model, we will consider the effect of the Higgs contributions to the ρ parameter at one-loop level. These contributions will be determined in the limit of the suppressed $Z - Z'$ mixing and the decoupling of the SM-like Higgs boson with other CP-even neutral Higgs bosons. As a consequence, the one-loop contribution of the SM-like Higgs boson to the ρ parameter is the same as in the SM. Excepting for the components of the scalar triplet ρ, the other heavy CP-even neutral Higgs bosons do not couple with the SM gauge bosons W and Z and thus they do not provide contributions to the ρ parameter. Contributions of the remaining Higgs bosons can be calculated using the results given in Ref. [38]. In particular, contributions of any Higgs bosons in our case to $\Delta\rho$ are determined as follows

$$\Delta\rho = \frac{\Pi_{WW}(0)}{M_W^2} - \frac{\Pi_{ZZ}(0)}{M_Z^2}, \tag{69}$$

where $\Pi_{WW}(0)$ and $\Pi_{ZZ}(0)$ are the coefficients of $-ig_{\mu\nu}$ in the vacuum-polarization amplitudes of charged and neutral W bosons and Z gauge bosons, respectively. Our case relates with only the contribution of "non-Higgs scalars" $\phi_{1,2}$ with masses $m_{1,2}$ and coupling

$$ic\phi_1^* \overleftrightarrow{\partial}_\mu \phi_2 V^\mu \equiv ic[\phi_1^* \partial_\mu \phi_2 - (\partial_\mu \phi_1^*)\phi_2]V^\mu, \quad (V = W, Z), \tag{70}$$

The corresponding contribution is

$$\Pi(\text{scalar}) = \frac{|c|^2}{16\pi^2} f_s(m_1, m_2), \tag{71}$$

where

$$\begin{aligned} f_s(m_1, m_2) = f_s(m_2, m_1) &= \frac{m_1^2 m_2^2}{m_1^2 - m_2^2} \ln\left[\frac{m_2^2}{m_1^2}\right] \\ &\quad + \frac{1}{2}(m_1^2 + m_2^2) \\ &= m_1^2 f_s(x) = m_1^2 \left(\frac{x \ln(x)}{1-x} + \frac{1+x}{2}\right), \\ x_{21} &\equiv \frac{m_2^2}{m_1^2}. \end{aligned} \tag{72}$$

The function in Eq. (72) satisfies $f_s(m_1, m_1) = \lim_{m_2 \to m_1} \times f_s(m_1, m_2) = 0$ and $f_s(m_1, m_2) > 0$ with $m_1 \neq m_2$. As a consequence, the charged Higgs bosons $\phi^\pm_{1,2,4}$ having vanishing Higgs-gauge couplings with other Higgs bosons give vanishing contributions to the ρ parameter. Nonvanishing contributions now may arise from the charged Higgs bosons $H^\pm_{1,2,3}$ corresponding to the basis $(\rho_1^\pm, \rho_3^\pm, \phi_3^\pm)$ and the CP-odd neutral Higgs relating with I_ρ. The relevant Lagrangian is

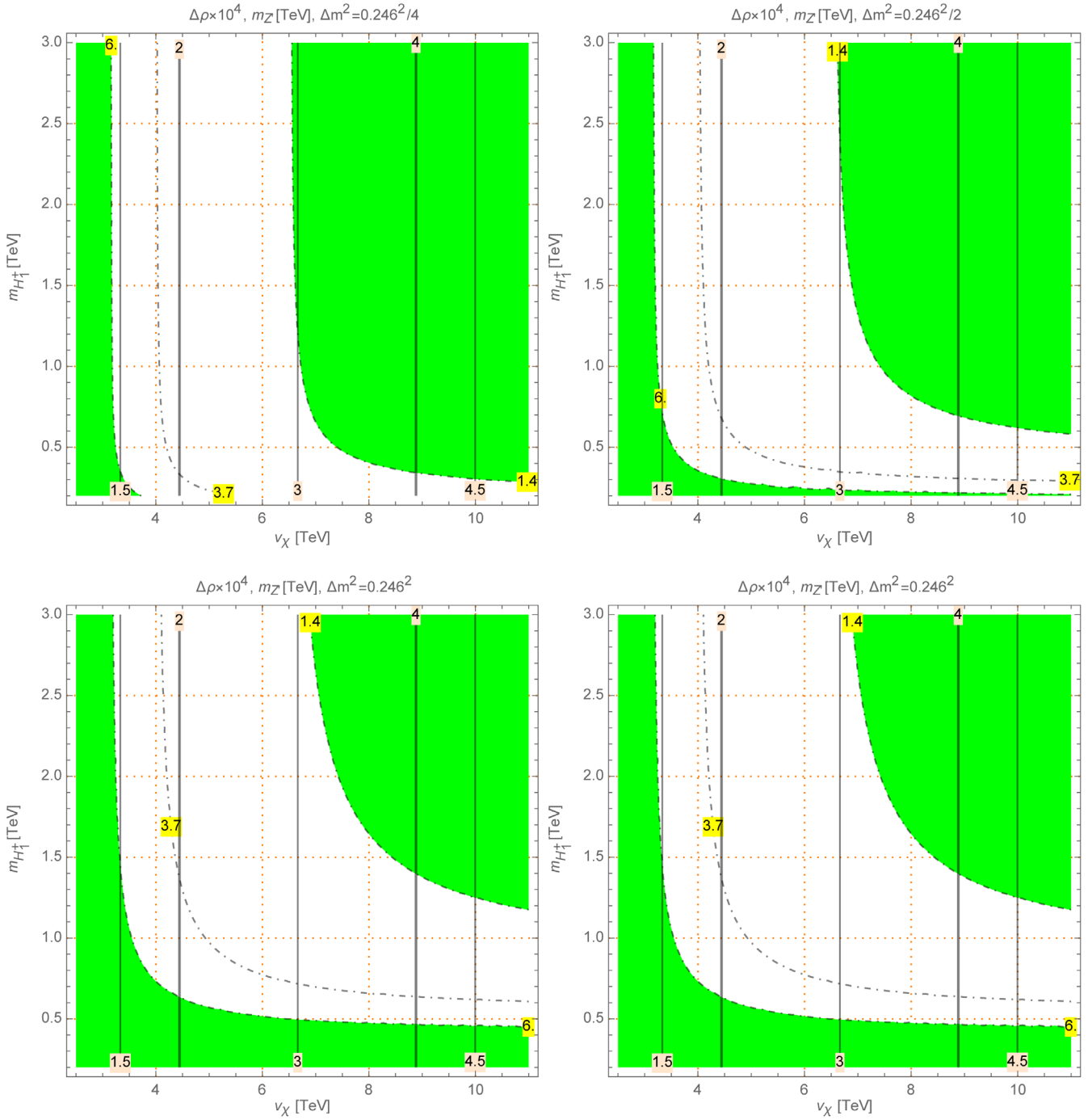

FIG. 2. Contour plots of the ρ parameter (dotted-dashed curves) and $M_{Z'}$ (black curves) as functions of v_χ and $m_{H_1^+}$. The green regions are excluded by the recent experimental constraint of the ρ.

$$\begin{aligned}\mathcal{L}_{VHH} &= (D_\mu\rho)^\dagger(D^\mu\rho) + (D_\mu\phi_3^+)^*(D^\mu\phi_3^+) \\ &\to \frac{ig}{2}Z^\mu\left[\frac{1-2s_W^2}{c_W}(\rho_1^-\overleftrightarrow{\partial}_\mu\rho_1^+) + \frac{-2s_W^2}{c_W}(\rho_3^-\overleftrightarrow{\partial}_\mu\rho_3^+) + \frac{-i}{c_W}(I_\rho\overleftrightarrow{\partial}_\mu R_\rho)\right] \\ &\quad + \frac{-igs_W^2}{c_W}Z^\mu(\phi_3^-\overleftrightarrow{\partial}_\mu\phi_3^+) + \left[-\frac{ig}{2}W^{+\mu}\rho_1^-(\overleftrightarrow{\partial}_\mu R_\rho - i\overleftrightarrow{\partial}_\mu I_\rho) + \text{H.c.}\right]. \end{aligned} \tag{73}$$

In the scalar-gauge interactions of Eq (73), only the last term contributes to $\Pi_{WW}(0)$, thus giving rise to a nonnegative contribution to the ρ parameter, which may make the allowed $M_{Z'}$ mass to move outside the excluded region recently reported by LHC searches [39]. On the contrary, all of the remaining terms contributing to $\Pi_{ZZ}(0)$, give nonpositive contributions to the ρ parameter. For illustration, we will consider a simple case where only positive contributions to the ρ parameter are kept, namely $\rho^{\pm}_{1,3} \equiv H^{\pm}_{1,3}$, $\phi^{\pm}_3 \equiv H^{\pm}_2$, $I_\rho \equiv A_2$ and R_ρ are mass eigenstates. Then, all contributions to $\Pi_{ZZ}(0)$ arising from the charged Higgs bosons are proportional to $f_s(m_s, m_s) = 0$ with $s = \rho^{\pm}_{1,3}$, $\phi^{\pm}_3$. In addition, the simplified condition (61) with $\lambda_1 \ll 1$ results in $m^2_{I_\rho} = m^2_{R_\rho}$, leading to a vanishing neutral Higgs boson contribution to $\Pi_{ZZ}(0)$: $f_s(m_{I_\rho}, m_{R_\rho}) = 0$. The only nonzero contribution has the form

$$\Delta\rho^H = \frac{g^2}{16\pi^2 m_W^2} f_s(m_{H_1^+}, m_{R_\rho}) = \frac{\sqrt{2}G_F}{16\pi^2} f_s(m_{H_1^+}, m_{R_\rho}), \tag{74}$$

where

$$\Delta m^2 \equiv m^2_{R_\rho} - m_{H_1^+} = -\frac{\lambda_9 v_\eta^2}{2} \sim \mathcal{O}(v_\eta^2). \tag{75}$$

Allowed regions of the parameter space for some specific values of Δm^2 are shown in Fig. 2. It can be seen that the large values of v_χ are still allowed, thus implying that no upper bounds are required. The allowed values of v_χ and $M_{Z'}$ strongly depend on the lower bound of $m_{H_1^\pm}$ and m_{R_ρ}, which may have previously reported from LHC searches. Unfortunately, the Higgs triplets ρ containing the neutral components ρ^0_2 with zero VEV, hence all of the three components of ρ do not couple to the two SM gauge bosons Z and W. This Higgs triplet also does not contribute to the SM-like Higgs boson. As a result, all of the Higgs bosons $H^{\pm}_1$, R_ρ, and I_ρ are not affected by the following decays searched by LHC: $H^{\pm}_1 \to W^{\pm}Z$, $W^{\pm}h$ and R_ρ, $I_\rho \to W^+W^-, ZZ, Zh$. These Higgs bosons do not couple with the SM quarks [19], cannot be produced at LHC from the recent channel searching [40]. Only the allowed tree level decays to two SM fermions are leptonic decays: $H^{\pm}_1 \to \nu_{2,3}\tau, \nu_{2,3}\mu$ and R_ρ, $I_\rho \to \bar{e}_i e_i$ $(i = 1, 2, 3)$, which are also searched by LHC, but the couplings of these Higgs with SM quarks are necessary to produce these Higgs bosons.

Because the above Higgs bosons have couplings with many new charged particles in the model under consideration, their one-loop level decays to photons may appear, thus making them interesting channels for their search at the LHC, in particular these charged Higgs bosons feature the following decay modes $H^{\pm}_1 \to W^{\pm}\gamma, R_\rho, I_\rho \to Z\gamma$ [41], and R_ρ, $I_\rho \to \gamma\gamma$ [42,43]. The heavy neutral Higgs boson masses are predicted to be at the TeV scale, which is outside the LHC excluded regions. Combined with the relation (75), the mass of the charged Higgs boson H^+_1 should also be at the TeV scale. From Fig. 2, we can see that $M_{Z'} \geq 4$ TeV is allowed if Δm^2 is large enough, for example $\Delta m^2 \geq (0.246\ \text{TeV})^2$.

V. CHARGED LEPTON FLAVOR VIOLATING DECAY CONSTRAINTS

In this section we will determine the constraints that the charged lepton flavor violating decays $\mu \to e\gamma$, $\tau \to \mu\gamma$ and $\tau \to e\gamma$ imposed on the parameter space of our model. As mentioned in Ref. [19], the sterile neutrino spectrum of the model is composed of two almost degenerate neutrinos with masses at the Fermi scale and four nearly degenerate neutrinos with TeV scale masses. These sterile neutrinos together with the heavy W' gauge boson induce the $l_i \to l_j\gamma$ decay at one loop level, whose branching ratio is given by: [44–46]:

$$\text{Br}(l_i \to l_j\gamma) = \frac{\alpha_W^3 s_W^2 m_{l_i}^5}{256\pi^2 m_{W'}^4 \Gamma_i} \left| 2G\left(\frac{m^2_{N_1}}{m^2_{W'}}\right) + 4G\left(\frac{m^2_{N_2}}{m^2_{W'}}\right) \right|^2,$$
$$G(x) = -\frac{2x^3 + 5x^2 - x}{4(1-x)^2} - \frac{3x^3}{2(1-x)^4}\ln x. \tag{76}$$

In our numerical analysis we have fixed $m_{N_1} = 100$ GeV and we have varied the W' gauge boson mass in the range $4\ \text{TeV} \lesssim m_{W'} \lesssim 5\ \text{TeV}$. We consider neutral heavy Z' gauge boson masses larger than 4 TeV to fulfill the bound arising from the experimental data on K, D and B meson mixings [28]. Figure 3 shows the allowed parameter space in the $m_{W'} - m_N$ plane consistent with the constraints arising from charged lepton flavor violating decays. As seen from Fig. 3, the obtained values for the branching ratio of $\mu \to e\gamma$ decay are below its experimental upper limit of 4.2×10^{-13} since these values are located in the range $3 \times 10^{-13} \lesssim \text{Br}(\mu \to e\gamma) \lesssim 4 \times 10^{-13}$, for sterile neutrino masses m_{N_2} lower than about 1.12 TeV. In the same region of parameter space, the obtained branching ratios for the $\tau \to \mu\gamma$ and $\tau \to e\gamma$ decays can reach

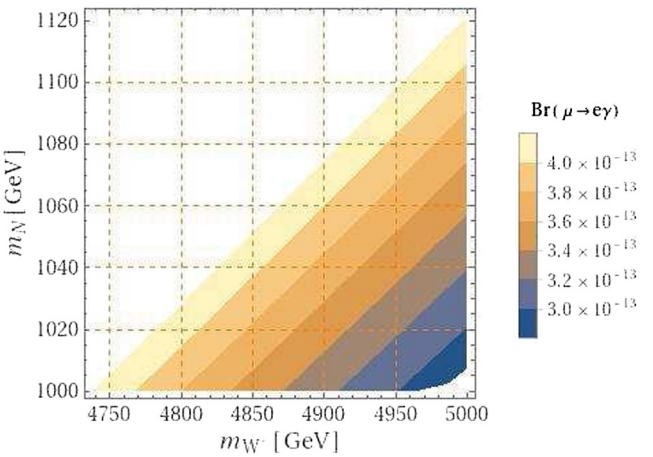

FIG. 3. Allowed parameter space in the $m_{W'} - m_N$ plane consistent with the LFV constraints.

values of the order of 10^{-13}, which is below their corresponding upper experimental bounds of 4.4×10^{-9} and 3.3×10^{-9}, respectively. Consequently, our model is compatible with the charged lepton flavor violating decay constraints provided that the sterile neutrinos are lighter than about 1.12 TeV.

VI. SEARCH FOR Z' AT LHC

In this section, we present two typical effects of the LHC, namely, production of single a particle in proton-proton collisions.

A. Phenomenology of Z' gauge boson

In what follows we proceed to compute the total cross section for the production of a heavy Z' gauge boson at the LHC via Drell-Yan mechanism. In our computation for the total cross section we consider the dominant contribution due to the parton distribution functions of the light up, down and strange quarks, so that the total cross section for the production of a Z' via quark antiquark annihilation in proton proton collisions with center of mass energy $\sqrt{S}$ takes the form:

$$\sigma^{(\mathrm{DrellYan})}_{pp\to Z'}(S) = \frac{g^2\pi}{6c_W^2 S}\left\{[(g'_{uL})^2+(g'_{uR})^2]\int_{\ln\sqrt{\frac{m^2_{Z'}}{S}}}^{-\ln\sqrt{\frac{m^2_{Z'}}{S}}} f_{p/u}\left(\sqrt{\frac{m^2_{Z'}}{S}}e^{y},\mu^2\right) f_{p/\bar{u}}\left(\sqrt{\frac{m^2_{Z'}}{S}}e^{-y},\mu^2\right)dy\right.$$
$$+[(g'_{dL})^2+(g'_{dR})^2]\int_{\ln\sqrt{\frac{m^2_{Z'}}{S}}}^{-\ln\sqrt{\frac{m^2_{Z'}}{S}}} f_{p/d}\left(\sqrt{\frac{m^2_{Z'}}{S}}e^{y},\mu^2\right) f_{p/\bar{d}}\left(\sqrt{\frac{m^2_{Z'}}{S}}e^{-y},\mu^2\right)dy$$
$$\left.+[(g'_{dL})^2+(g'_{dR})^2]\int_{\ln\sqrt{\frac{m^2_{Z'}}{S}}}^{-\ln\sqrt{\frac{m^2_{Z'}}{S}}} f_{p/s}\left(\sqrt{\frac{m^2_{Z'}}{S}}e^{y},\mu^2\right) f_{p/\bar{s}}\left(\sqrt{\frac{m^2_{Z'}}{S}}e^{-y},\mu^2\right)dy\right\}$$

Figure 4 displays the Z' total production cross section at the LHC via Drell-Yan mechanism at the LHC for $\sqrt{S} = 13$ TeV and as a function of the Z' mass, which is taken to range from 4 TeV up to 5 TeV. We consider neutral heavy Z' gauge boson masses larger than 4 TeV to fulfill the bound arising from the experimental data on K, D, and B meson mixings [28]. For such as a region of Z' masses we find that the total production cross section ranges from 85 fb up to 10 fb. The heavy neutral Z' gauge boson after being produced it will decay into pair of SM particles, with dominant decay mode into quark-antiquark pairs as shown in detail in Refs. [24,47]. The two body decays of the Z' gauge boson in 3-3-1 models have been studied in details in Refs. [47]. In particular, in Ref. [47] it has been shown the Z' decays into a lepton pair in 3-3-1 models have branching ratios of the order of 10^{-2}, which implies that the total LHC cross section for the $pp \to Z' \to l^+l^-$ resonant production at $\sqrt{S} = 13$ TeV will be of the order of 1 fb for a 4 TeV Z' gauge boson, which is below its corresponding lower experimental limit arising from LHC searches [39]. On the other hand, at the proposed energy upgrade of the LHC at 28 TeV center of mass energy, the total cross section for the Drell-Yan production of a heavy Z' neutral gauge boson gets significantly enhanced reaching values ranging from 2.5 pb up to 0.7 pb, as indicated in Fig. 5. Consequently, the LHC cross section for the $pp \to Z' \to l^+l^-$ resonant production at $\sqrt{S} = 28$ TeV

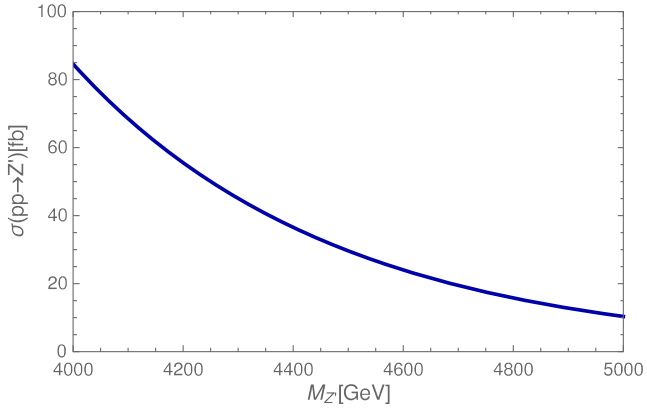

FIG. 4. Total cross section for the Z' production via Drell-Yan mechanism at the LHC for $\sqrt{S} = 13$ TeV and as a function of the Z' mass.

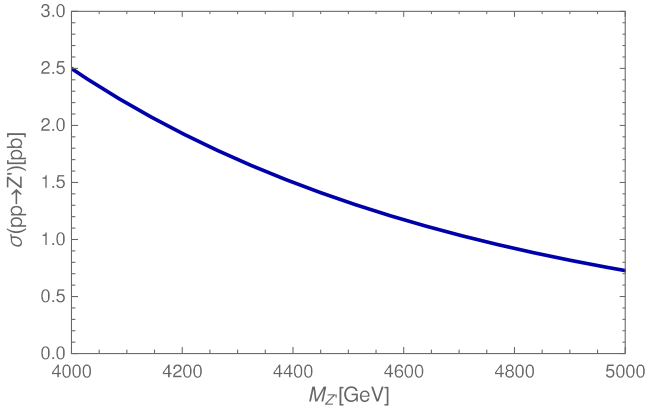

FIG. 5. Total cross section for the Z' production via Drell-Yan mechanism at the proposed energy upgrade of the LHC with $\sqrt{S} = 28$ TeV as a function of the Z' mass.

will be of the order of 10^{-2} pb for a 4 TeV Z' gauge boson, which corresponds to the order of magnitude of its corresponding lower experimental limit arising from LHC searches [39].

B. Phenomenology of H_4 heavy Higgs boson

In what follows we proceed to compute the LHC production cross section of the singly heavy scalar H_4. Let us note that the singly heavy scalar H_4 is mainly produced via gluon fusion mechanism mediated by a triangular loop of the heavy exotic quarks T, J_1, and J_2. Thus, the total cross section for the production of the heavy scalar H_4 through gluon fusion mechanism in proton proton collisions with center of mass energy $\sqrt{S}$ takes the form:

$$\sigma_{pp\to gg\to H_4}(S) = \frac{\alpha_S^2 m_{H_4}^2 |(R_{CP\text{even}3})_{22}|^2}{64\pi v_\chi^2 S}\left[I\left(\frac{m_{H_4}^2}{m_T^2}\right) + I\left(\frac{m_{H_4}^2}{m_{J_1}^2}\right) + I\left(\frac{m_{H_4}^2}{m_{J_2}^2}\right)\right] \times \int_{\ln\sqrt{\frac{m_{H_4}^2}{S}}}^{-\ln\sqrt{\frac{m_{H_4}^2}{S}}} f_{p/g}\left(\sqrt{\frac{m_{H_4}^2}{S}}e^{y},\mu^2\right) f_{p/g}\left(\sqrt{\frac{m_{H_4}^2}{S}}e^{-y},\mu^2\right) dy$$

where $f_{p/g}(x_1,\mu^2)$ and $f_{p/g}(x_2,\mu^2)$ are the distributions of gluons in the proton which carry momentum fractions x_1 and x_2 of the proton, respectively. Furthermore $\mu = m_{H_4}$ is the factorization scale and $I(z)$ is given by:

$$I(z) = \int_0^1 dx \int_0^{1-x} dy \frac{1-4xy}{1-zxy}. \tag{77}$$

Figure 6 displays the H_4 total production cross section at the LHC via gluon fusion mechanism for $\sqrt{S} = 13$ TeV, as a function of the $SU(3)_L \times U(1)_X$ symmetry breaking scale v_χ, which is taken to range from 10 TeV up to 20 TeV. The aforementioned range of values for the $SU(3)_L \times U(1)_X$ symmetry breaking scale v_χ corresponds to a heavy scalar mass m_{H_4} varying between 4.4 TeV and 8.9 TeV. Considering the mass of the heavy scalar field H_4 in the range 8 TeV $\lesssim M_{H_4} \lesssim$ 8.9 TeV, it is reasonable to assume that it will have dominant decay modes into $W'W'$ and $Z'Z'$ heavy gauge boson pairs. On the other hand, for a heavy scalar field H_4 with mass in the range 4.4 TeV $\lesssim M_{H_4} \lesssim$ 8 TeV, based on Ref. [48], it is reasonable to assume that its dominant decay mode will be on $t\bar{t}$ pair. Furthermore, in the region of H_4 masses considered in our analysis, the H_4 decay into exotic quark pairs will be kinematically forbidden for exotic quark Yukawa couplings of order unity. Note that we have chosen values for v_χ larger than 10 TeV, which corresponds to a Z' gauge boson heavier than 4 TeV, which is required to guarantee the consistency of 331 models with the experimental data on K, D, and B meson mixings [28]. Here, for the sake of simplicity we have restricted to the simplified scenario described by Eq. (62) and we have chosen the exotic quark Yukawa couplings equal to unity, i.e., $y^{(T)} = y^{(J_1)} = y^{(J_2)} = 1$. In addition, the top quark mass has been taken to be equal to $m_t = 173$ GeV. We find that the total cross section for the production of the H_4 scalar at the LHC takes a value close to about 10^{-4} fb for the lower bound of 10 TeV of the

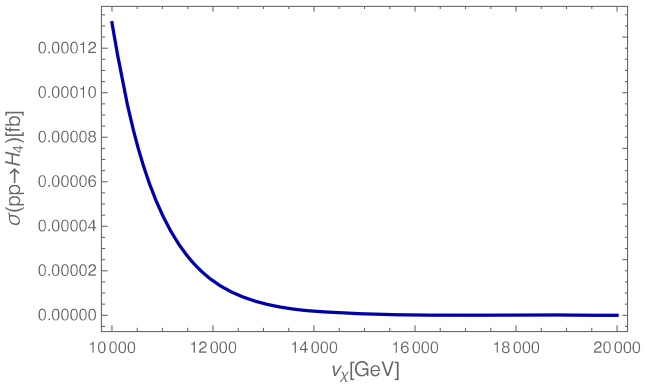

FIG. 6. Total cross section for the H_4 production via gluon fusion mechanism at the LHC for $\sqrt{S} = 13$ TeV and as a function of the $SU(3)_L \times U(1)_X$ symmetry breaking scale v_χ for the simplified scenario described in Eq. (62).

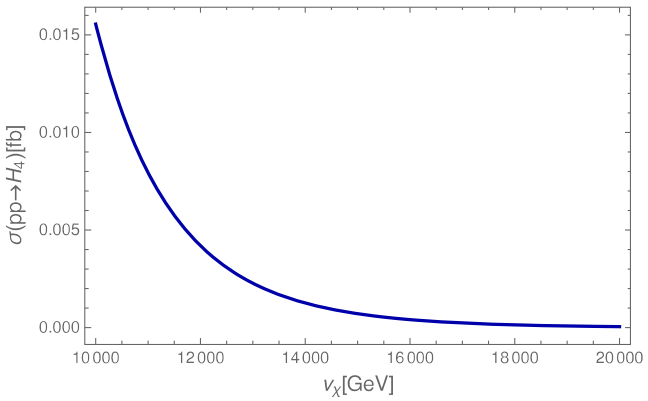

FIG. 7. Total cross section for the H_4 production via gluon fusion mechanism at the proposed energy upgrade of the LHC with $\sqrt{S} = 28$ TeV as a function of the $SU(3)_L \times U(1)_X$ symmetry breaking scale v_χ for the simplified scenario described in Eq. (62).

$SU(3)_L \times U(1)_X$ symmetry breaking scale v_χ arising from the experimental data on K, D, and B meson mixings [28] and decreases when v_χ takes larger values. We see that the total cross section at the LHC for the H_4 production via gluon fusion mechanism is small to give rise to a signal for the allowed values of the $SU(3)_L \times U(1)_X$ symmetry breaking scale v_χ. A similar situation happens at the proposed energy upgrade of the LHC with $\sqrt{S} = 28$ TeV, where this total cross section takes a value of 1.6×10^{-2} fb for $v_\chi = 10$ TeV as shown in Fig. 7. Because of the very small H_4 production cross section, we do not perform a detailed study of its decay modes. It is worth mentioning that the smoking gun signatures of the model under consideration will be the Z' production and the charged lepton flavor violating decay $\mu \to e\gamma$, whose observation will be crucial to assess to viability of this model.

VII. DARK MATTER RELIC DENSITY

In this section we provide a discussion of the implications of our model for DM, assuming that the DM candidate is a scalar. Let us recall that our goal in this section is to provide an estimate of the DM relic density in our model, under some simplifying assumptions motivated by the large number of scalar fields of the model. We do not intend to provide a sophisticated analysis of the DM constraints of the model under consideration, which is beyond the scope of the present paper. We just intend to show that our model can accommodate the observed value of the DM relic density, by having a scalar DM candidate with a mass in the TeV range and a quartic scalar coupling of the order unity, within the perturbative regime. We start by surveying the possible scalar DM candidates in the model. Considering that the Z_4 symmetry is preserved and taking into account the scalar assignments under this symmetry, given by Eq. (1), we can assign this role to either any of the $SU(3)_L$ scalar singlets, i.e., $Re\varphi_n^0$ and $Im\varphi_n^0$ $(n = 1, 2)$. In this work we assume that the $\varphi_I = Im\varphi_1^0$ is the lightest among the $Re\varphi_n^0$ and $Im\varphi_n^0$ $(n = 1, 2)$ scalar fields and also lighter than the exotic charged fermions, as well as lighter than Ψ_R, thus implying that its tree-level decays are kinematically forbidden. Consequently, in this mass range the $Im\varphi_1^0$ scalar field is stable.

The relic density is given by (cf. Ref. [30,49])

$$\Omega h^2 = \frac{0.1pb}{\langle\sigma v\rangle}, \qquad \langle\sigma v\rangle = \frac{A}{n_{\rm eq}^2} = \frac{\frac{T}{32\pi^4}\int_{4m_\varphi^2}^{\infty}\sum_{p=W,Z,t,b,h} g_p^2 \frac{s\sqrt{s-4m_\varphi^2}}{2} v_{\rm rel}\sigma(\varphi\varphi \to p\bar{p})K_1(\frac{\sqrt{s}}{T})ds}{(\frac{T}{2\pi^2}\sum_{p=W,Z,t,b,h} g_p m_\varphi^2 K_2(\frac{m_\varphi}{T}))^2}, \tag{78}$$

where $\langle\sigma v\rangle$ is the thermally averaged annihilation cross section, A is the total annihilation rate per unit volume at temperature T, and $n_{\rm eq}$ is the equilibrium value of the particle density. Furthermore, K_1 and K_2 are modified Bessel functions of the second kind and order 1 and 2, respectively [49] and $m_\varphi = m_{{\rm Im}\varphi}$. Let us note that we assume that our scalar DM candidate is a stable weakly interacting particle (WIMP) with annihilation cross sections mediated by electroweak interactions mainly through the Higgs field. In addition we assume that the decoupling of the nonrelativistic WIMP of our model is supposed to happen at a very low temperature. Because of this reason, for the computation of the relic density, we take $T = m_\varphi/20$ as in Ref. [49], corresponding to a typical freeze-out temperature. We assume that our DM candidate φ annihilates mainly into WW, ZZ, $t\bar{t}$, $b\bar{b}$, and hh, with annihilation cross sections given by the following relations [50]:

$$\begin{aligned}
v_{\rm rel}\sigma(\varphi_I\varphi_I \to WW) &= \frac{\lambda_{h^2\varphi^2}^2}{8\pi}\frac{s\left(1+\frac{12m_W^4}{s^2}-\frac{4m_W^2}{s}\right)}{(s-m_h^2)^2+m_h^2\Gamma_h^2}\sqrt{1-\frac{4m_W^2}{s}},\\
v_{\rm rel}\sigma(\varphi_I\varphi_I \to ZZ) &= \frac{\lambda_{h^2\varphi^2}^2}{16\pi}\frac{s\left(1+\frac{12m_Z^4}{s^2}-\frac{4m_Z^2}{s}\right)}{(s-m_h^2)^2+m_h^2\Gamma_h^2}\sqrt{1-\frac{4m_Z^2}{s}},\\
v_{\rm rel}\sigma(\varphi_I\varphi_I \to q\bar{q}) &= \frac{N_c\lambda_{h^2\varphi^2}^2 m_q^2}{4\pi}\frac{\sqrt{\left(1-\frac{4m_f^2}{s}\right)^3}}{(s-m_h^2)^2+m_h^2\Gamma_h^2},\\
v_{\rm rel}\sigma(\varphi_I\varphi_I \to hh) &= \frac{\lambda_{h^2\varphi^2}^2}{16\pi s}\left(1+\frac{3m_h^2}{s-m_h^2}-\frac{4\lambda_{h^2\varphi^2}v^2}{s-2m_h^2}\right)^2\sqrt{1-\frac{4m_h^2}{s}},
\end{aligned} \tag{79}$$

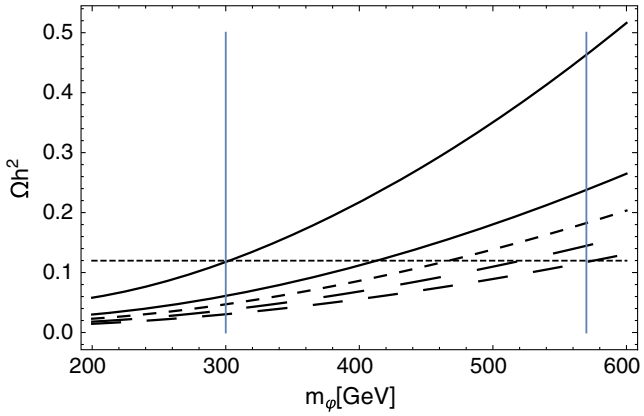

FIG. 8. Relic density Ωh^2, as a function of the mass m_φ of the φ scalar field, for several values of the quartic scalar coupling $\lambda_{h^2\varphi^2}$. The curves from top to bottom correspond to $\lambda_{h^2\varphi^2} = 0.5$, 0.7, 0.8, 0.9, 1, respectively. The horizontal line shows the observed value $\Omega h^2 = 0.1198$ [54] for the relic density. The vertical lines correspond to the obtained lower and upper limits 300 GeV and 570 GeV, respectively, of the mass m_φ of the scalar dark matter candidate consistent with the experimental measurement of the dark matter relic density.

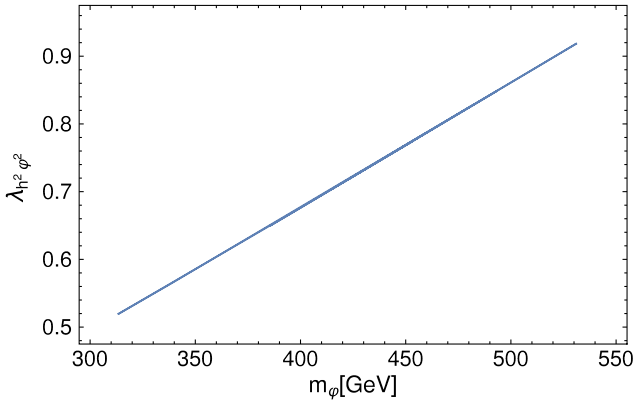

FIG. 9. Correlation between the quartic scalar coupling and the mass m_φ of the scalar DM candidate φ, consistent with the experimental value $\Omega h^2 = 0.1198$ for the relic density.

where $\sqrt{s}$ is the center-of-mass energy, $N_c = 3$ is the color factor, $m_h = 125.7$ GeV and $\Gamma_h = 4.1$ MeV are the SM Higgs boson h mass and its total decay width, respectively. Note that we have worked on the decoupling limit where the couplings of the 126 GeV Higgs boson to SM particles and its self-couplings correspond to the SM expectation.

The vacuum stability and tree level unitarity constraints of the scalar potential are [51–53]

$$\lambda_{h^4} > 0, \qquad \lambda_{\varphi^4} > 0, \qquad \lambda^2_{h^2\varphi^2} < \frac{2}{3}\lambda_{h^4}\lambda_{\varphi^4}. \tag{80}$$

$$\lambda_{\varphi^4} < 8\pi, \qquad \lambda_{h^2\varphi^2} < 4\pi. \tag{81}$$

The dark matter relic density as a function of the mass m_φ of the scalar field φ_I is shown in Fig. 8, for several values of the quartic scalar coupling $\lambda^2_{h^2\varphi^2}$, set to be equal to 0.7, 0.8 and 0.9 (from top to bottom). The horizontal line corresponds to the experimental value $\Omega h^2 = 0.1198$ for the relic density. We found that the DM relic density constraint gives rise to a linear correlation between the quartic scalar coupling $\lambda_{h^2\varphi^2}$ and the mass m_φ of the scalar DM candidate φ_I, as indicated in Fig. 9.

We find that we can reproduce the experimental value $\Omega h^2 = 0.1198 \pm 0.0026$ [54] of the DM relic density, when the mass m_φ of the scalar field φ_I is in the range $300\ \text{GeV} \lesssim m_\varphi \lesssim 570\ \text{GeV}$, for a quartic scalar coupling $\lambda_{h^2\varphi^2}$ in the window $0.5 \lesssim \lambda_{h^2\varphi^2} \lesssim 1$, which is consistent with the vacuum stability and unitarity constraints shown in Eqs. (80) and (81). Note that our range of values chosen for the quartic scalar coupling $\lambda_{h^2\varphi^2}$ also allow the extrapolation of our model at high energy scales as well as the preservation of perturbativity at one loop level.

VIII. CONCLUSIONS

We have studied some phenomenological aspects of the extended inert 331 model, which incorporates the mechanism of sequential loop-generation of the SM fermion masses, explaining the observed strong hierarchies between them as well as the corresponding mixing parameters. A particular emphasis has been made on analyzing the constraints arising from the experimental data on the ρ parameter, as well as those ones resulting from the charged lepton flavor violating process $\mu \to e\gamma$ and dark matter. Furthermore, we have studied the production of the heavy Z' gauge boson in proton-proton collisions via the Drell-Yan mechanism. We found that the corresponding total cross section at the LHC ranges from 85 fb up to 10 fb when the Z' gauge boson mass is varied within a 4–5 TeV interval. The Z' production cross section gets significantly enhanced at the proposed energy upgrade of the LHC with $\sqrt{S} = 28$ TeV reaching the typical values of 2.5–0.7 pb. From these results we find that the $pp \to Z' \to l^+l^-$ resonant production cross section reach values of about 1 fb and 10^{-2} pb at $M_{Z'} = 4$ TeV, for $\sqrt{S} = 14$ TeV and $\sqrt{S} = 28$ TeV, respectively. These obtained values for the $pp \to Z' \to l^+l^-$ resonant production cross sections are below and of the same order of magnitude of its corresponding lower experimental limit arising from LHC searches, for $\sqrt{S} = 13$ TeV and $\sqrt{S} = 28$ TeV, respectively. Besides that, we have found that Z' gauge bosons heavier than about 4 TeV comply with the experimental constraints on the oblique ρ parameter as well as with the collider constraints. In addition, we have found that the constraint on the charged lepton flavor violating decay $\mu \to e\gamma$ set the sterile neutrino masses to be lighter than about 1.12 TeV. We have found that the obtained values of the branching ratio for the $\mu \to e\gamma$ decay are located in the

range $3 \times 10^{-13} \lesssim \mathrm{Br}(\mu \to e\gamma) \lesssim 4 \times 10^{-13}$, whereas the obtained branching ratios for the $\tau \to \mu\gamma$ and $\tau \to e\gamma$ decays can reach values of the order of 10^{-13}. Consequently, our model predicts charged lepton flavor violating decays within the reach of future experimental sensitivity. We found that the total cross section for the production of the H_4 scalar at the LHC with $\sqrt{S} = 13$ TeV takes a value close to about 10^{-4} fb for the lower bound of 10 TeV of the $SU(3)_L \times U(1)_X$ symmetry breaking scale v_χ required by the consistency of the ρ parameter with the experimental data. This value is increased to 1.6×10^{-2} fb at the proposed energy upgrade of the LHC with $\sqrt{S} = 28$ TeV, thus implying that the total cross section at the LHC for the H_4 production via gluon fusion mechanism is very small to give rise to a signal for the allowed values of the $SU(3)_L \times U(1)_X$ symmetry breaking scale v_χ even at the proposed energy upgrade of the LHC. We also analyzed in detail the scalar potential and the gauge sector of the model.

The general Higgs sector is separated into two parts. The first part consists of lepton number conserving terms and the second one contains lepton number violating couplings. The first part of potential was considered in details and the SM Higgs boson was derived and as expected, mainly arises from η_1^0. We have shown that the whole scalar potential, excepting its CP-even sector, has a quite similar situation since the resulting physical scalar mass spectrum is similar in both cases. The scalar spectrum contains enough number of Goldstone bosons for massive gauge bosons. In the CP-odd scalar sector, there are four massive bosons and one of them is a DM candidate. The CP-even scalar mass spectrum consists of seven massive fields including the SM Higgs boson and a DM candidate. The singly electrically charged Higgs boson sector contains six massive fields. Two of them have masses at the electroweak scale and the remaining one has a mass around 3.5 TeV. The masses for the three charged bosons ϕ_i^+, $i = 1, 2, 4$ are not fixed. The scalar potential contains a Majoron but it is harmless, because it is a scalar singlet. Due to the unbroken Z_4 symmetry our model has the stable scalar dark matter candidates $Re\varphi_n^0$ and $Im\varphi_n^0$ ($n = 1, 2$) and the fermionic dark matter candidate Ψ_R. In this work we assume that $\varphi_I = Im\varphi_1^0$ is the lightest among the $Re\varphi_n^0$ and $Im\varphi_n^0$ ($n = 1, 2$) scalar fields and also lighter than the exotic charged fermions and than Ψ_R, which implies that it is stable and thus it is the dark matter candidate considered in this work. To reproduce the dark matter relic density, the mass of the scalar dark matter candidate has to be in the range $300\ \mathrm{GeV} \lesssim m_\varphi \lesssim 570\ \mathrm{GeV}$, for a quartic scalar coupling $\lambda_{h^2\varphi^2}$ in the window $0.5 \lesssim \lambda_{h^2\varphi^2} \lesssim 1$. In addition, it has been shown in Ref. [19] that requiring that the DM candidate φ^0 lifetime be greater than the universe lifetime $\tau_u \approx 13.8$ Gyr and assuming $m_{\varphi^0} \sim 1$ TeV, we estimate the cutoff scale of our model $\Lambda > 3 \times 10^{10}$ GeV. Thus we conclude that under the above specified conditions the model contains viable fermionic Ψ_R and scalar φ^0 DM candidates. A sophisticated analysis of the DM constraints of our model is beyond the scope of the present paper and is left for future studies.

ACKNOWLEDGMENTS

This research has been financially supported by Fondecyt (Chile), Grant No. 1170803, CONICYT PIA/Basal FB0821, the Vietnam National Foundation for Science and Technology Development (NAFOSTED) under Grant No. 103.01-2017.356. H. N. L. is very grateful to the Bogoliubov Laboratory for Theoretical Physics, JINR, Dubna, Russia for the warm hospitality during his visit.

APPENDIX: THE SCALAR POTENTIAL

The renormalizable potential contain three parts: the first one invariant under group $\mathcal{G}$ in (1) is given by

$$
\begin{aligned}
V_{\mathrm{LNC}} = {} & \mu_\chi^2 \chi^\dagger\chi + \mu_\rho^2 \rho^\dagger\rho + \mu_\eta^2 \eta^\dagger\eta + \sum_{i=1}^{4} \mu_{\phi_i^+}^2 \phi_i^+ \phi_i^- + \sum_{i=1}^{2} \mu_{\varphi_i}^2 \varphi_i^0 \varphi_i^{0*} + \mu_\xi^2 \xi^{0*}\xi^0 \\
& + \chi^\dagger\chi(\lambda_{13}\chi^\dagger\chi + \lambda_{18}\rho^\dagger\rho + \lambda_5 \eta^\dagger\eta) + \rho^\dagger\rho(\lambda_{14}\rho^\dagger\rho + \lambda_6\eta^\dagger\eta) + \lambda_{17}(\eta^\dagger\eta)^2 \\
& + \lambda_7(\chi^\dagger\rho)(\rho^\dagger\chi) + \lambda_8(\chi^\dagger\eta)(\eta^\dagger\chi) + \lambda_9(\rho^\dagger\eta)(\eta^\dagger\rho) \\
& + \chi^\dagger\chi\left(\sum_{i=1}^{4} \lambda_i^{\chi\phi} \phi_i^+\phi_i^- + \sum_{i=1}^{2} \lambda_i^{\chi\varphi} \varphi_i^0 \varphi_i^{0*} + \lambda_{\chi\xi}\xi^{0*}\xi^0\right) \\
& + \rho^\dagger\rho\left(\sum_{i=1}^{4} \lambda_i^{\rho\phi} \phi_i^+\phi_i^- + \sum_{i=1}^{2} \lambda_i^{\rho\varphi} \varphi_i^0 \varphi_i^{0*} + \lambda_{\rho\xi}\xi^{0*}\xi^0\right) \\
& + \eta^\dagger\eta\left(\sum_{i=1}^{4} \lambda_i^{\eta\phi} \phi_i^+\phi_i^- + \sum_{i=1}^{2} \lambda_i^{\eta\varphi} \varphi_i^0 \varphi_i^{0*} + \lambda_{\eta\xi}\xi^{0*}\xi^0\right)
\end{aligned}
$$

$$
\begin{aligned}
&+\sum_{i=1}^{4}\phi_i^+\phi_i^-\left(\sum_{j=1}^{4}\lambda_{ij}^{\phi\phi}\phi_j^+\phi_j^-+\sum_{j=1}^{2}\lambda_{ij}^{\phi\varphi}\varphi_j^0\varphi_j^{0*}+\lambda_i^{\phi\xi}\xi^{0*}\xi^0\right)\\
&+\sum_{i=1}^{2}\varphi_i^0\varphi_i^{0*}\left(\sum_{j=1}^{2}\lambda_{ij}^{\varphi\varphi}\varphi_j^0\varphi_j^{0*}+\lambda_i^{\varphi\xi}\xi^{0*}\xi^0\right)+\lambda_\xi(\xi^{0*}\xi^0)^2\\
&+\Big\{\lambda_{10}(\phi_2^+)^2(\phi_3^-)^2+\lambda_{11}(\phi_2^+)^2(\phi_4^-)^2+\lambda_{12}(\phi_3^+)^2(\phi_4^-)^2+w_1(\varphi_2^0)^2\varphi_1^0+w_2\chi^\dagger\rho\phi_3^-+w_3\eta^\dagger\chi\xi^0\\
&+w_4(\varphi_2^0)^2\varphi_1^{0*}+w_5\phi_3^+\phi_4^-\varphi_1^0+w_6\phi_3^+\phi_4^-\varphi_1^{0*}+\chi\rho\eta(\lambda_1\varphi_1^0+\lambda_2\varphi_1^{0*})+\chi^\dagger\rho\phi_4^-(\lambda_{15}\varphi_1^0+\lambda_{16}\varphi_1^{0*})\\
&+\lambda_3\eta^\dagger\rho\phi_3^-\xi^0+\lambda_4\phi_1^+\phi_2^-\varphi_2^0\xi^0+(\lambda_{19}\phi_3^-\phi_4^++\lambda_{20}\phi_3^+\phi_4^-)(\varphi_2^0)^2+\lambda_{21}(\varphi_1^0)^3\varphi_1^{0*}\\
&+(\lambda_{22}\chi^\dagger\chi+\lambda_{23}\rho^\dagger\rho+\lambda_{24}\eta^\dagger\eta+\sum_{i=1}^{4}\lambda_{61i}\phi_i^+\phi_i^-+\sum_{i=1}^{2}\lambda_{62i}\varphi_i^0\varphi_i^{0*}+\lambda_{25}\xi^{0*}\xi^0)(\varphi_1^0)^2+\text{H.c.}\Big\}. \qquad \text{(A1)}
\end{aligned}
$$

The second part is a lepton number violating one (the subgroup $U(1)_{L_g}$ is violated)

$$
\begin{aligned}
V_{\text{LNV}}&=\mu_{\chi\eta}^2(\chi^\dagger\eta+\eta^\dagger\chi)+[\lambda_{26}(\chi^\dagger\chi)+\lambda_{27}(\rho^\dagger\rho)+\lambda_{28}(\eta^\dagger\eta)](\chi^\dagger\eta+\eta^\dagger\chi)\\
&+\lambda_{29}[(\chi^\dagger\eta)^2+(\eta^\dagger\chi)^2]+\lambda_{30}[(\eta^\dagger\rho)(\rho^\dagger\chi)+(\chi^\dagger\rho)(\rho^\dagger\eta)]\\
&+\Big\{\xi^0\left(w_7\chi^\dagger\chi+w_8\rho^\dagger\rho+w_9\eta^\dagger\eta+\sum_{i=1}^{4}w_{2i}\phi_i^+\phi_i^-+\sum_{i=1}^{2}w_{3i}\varphi_i^0\varphi_i^{0*}+w_{10}\xi^{0*}\xi^0\right)\\
&+\xi^0[w_{11}\chi^\dagger\eta+w_{12}(\varphi_1^0)^2+w_{13}(\varphi_1^{0*})^2+w_{14}(\xi^0)^2]+w_{15}\eta^\dagger\rho\phi_3^-+w_{16}\phi_2^-\phi_1^+\varphi_2^0\\
&+(\xi^0)^2\left[\lambda_{31}\chi^\dagger\chi+\lambda_{32}\rho^\dagger\rho+\lambda_{33}\eta^\dagger\eta+\sum_{i=1}^{4}\lambda_{63i}\phi_i^+\phi_i^-+\sum_{i=1}^{2}\lambda_{64i}\varphi_i^0\varphi_i^{0*}+\lambda_{34}\xi^{0*}\xi^0+\lambda_{35}(\varphi_1^0)^2+\lambda_{36}(\varphi_1^{0*})^2\right]\\
&+\chi^\dagger\eta\left[\sum_{i=1}^{4}\lambda_{65i}\phi_i^+\phi_i^-+\sum_{i=1}^{2}\lambda_{66i}\varphi_i^0\varphi_i^{0*}+\lambda_{37}\xi^{0*}\xi^0+\lambda_{38}(\varphi_1^0)^2+\lambda_{39}(\varphi_1^{0*})^2+\lambda_{40}(\xi^0)^2+\lambda_{41}(\xi^{0*})^2\right]\\
&+\eta^\dagger\rho(\lambda_{42}\phi_4^-\varphi_1^0+\lambda_{43}\phi_4^-\varphi_1^{0*}+\lambda_{44}\phi_3^-\xi^{0*})+\rho^\dagger\chi\phi_3^+(\lambda_{45}\xi^0+\lambda_{46}\xi^{0*})\\
&+\lambda_{47}(\phi_1^+)^2\phi_3^-\phi_4^-+\phi_1^+\phi_2^-(\lambda_{48}\varphi_1^0\varphi_2^{0*}+\lambda_{49}\varphi_1^{0*}\varphi_2^{0*}+\lambda_{50}\varphi_2^0\xi^{0*})\\
&+\phi_3^+\phi_4^-(\lambda_{51}\varphi_1^0\xi^0+\lambda_{52}\varphi_1^0\xi^{0*}+\lambda_{53}\varphi_1^{0*}\xi^0+\lambda_{54}\varphi_1^{0*}\xi^{0*})\\
&+(\varphi_2^0)^2(\lambda_{55}\varphi_1^0\xi^0+\lambda_{56}\varphi_1^0\xi^{0*}+\lambda_{57}\varphi_1^{0*}\xi^0+\lambda_{58}\varphi_1^{0*}\xi^{0*})+\text{H.c.}\Big\} \qquad \text{(A2)}
\end{aligned}
$$

The last part which breaks softly $Z_4\times Z_2$, is given by

$$
\begin{aligned}
L_{\text{gsoft}}^{\text{scalars}}&=\mu_4^2\varphi_1^0\varphi_2^0+\mu_6^2\varphi_1^0\varphi_2^{0*}+\mu_1^2(\varphi_2^0)^2+\mu_2^2\phi_2^+\phi_3^-\\
&+\mu_5^2\phi_2^+\phi_4^-+\mu_3^2\phi_3^+\phi_4^-+\text{H.c.} \qquad \text{(A3)}
\end{aligned}
$$

The total potential is composed of three above mentioned parts

$$
V=V_{\text{LNC}}+V_{\text{LNV}}+\mathcal{L}_{\text{soft}}^{\text{scalars}}. \qquad \text{(A4)}
$$

The scalar interactions needed for quark and charged lepton mass generation, read as follows

$$
\begin{aligned}
L_{\text{Higgsqcl}}&=\lambda_1\chi\rho\eta\varphi_1^0+\lambda_3\eta^\dagger\rho\phi_3^-\xi^0+\lambda_4\phi_1^+\phi_2^-\varphi_2^0\xi^0\\
&+w_1(\varphi_2^0)^2\varphi_1^0+w_2\chi^\dagger\rho\phi_3^-+\text{H.c.} \qquad \text{(A5)}
\end{aligned}
$$

For the neutrino mass generation, beside the first term in (A5), the additional part is given as

$$
\begin{aligned}
L_{\text{Higgsneutrino}}&=\lambda_{13}(\chi^\dagger\chi)^2+\lambda_5(\chi^\dagger\chi)(\eta^\dagger\eta)\\
&+[\lambda_{27}(\rho^\dagger\rho)(\chi^\dagger\eta+\eta^\dagger\chi)+\mu_3^2\phi_4^-\phi_3^++\text{H.c}]. \qquad \text{(A6)}
\end{aligned}
$$

It is worth mentioning that for the generation of masses for quark and charged lepton, only terms in the conserving part V_{LNC} are enough, while for the generation of the light active neutrino masses, one needs the lepton number violating scalar interactions of V_{LNV} as well as the softly breaking part $\mathcal{L}_{\text{soft}}^{\text{scalars}}$ [the last term in (A6)] of the scalar potential.

[1] C. D. Froggatt and H. B. Nielsen, Hierarchy of quark masses, Cabibbo angles and CP violation, Nucl. Phys. **B147**, 277 (1979).

[2] A. E. Cárcamo Hernández, S. Kovalenko, and I. Schmidt, Radiatively generated hierarchy of lepton and quark masses, J. High Energy Phys. 02 (2017) 125.

[3] M. Singer, J. W. F. Valle, and J. Schechter, Canonical neutral current predictions from the weak electromagnetic gauge group $SU(3) \times U(1)$, Phys. Rev. D **22**, 738 (1980).

[4] J. W. F. Valle and M. Singer, Lepton number violation with quasi dirac neutrinos, Phys. Rev. D **28**, 540 (1983).

[5] F. Pisano and V. Pleitez, An $SU(3) \times U(1)$ model for electroweak interactions, Phys. Rev. D **46**, 410 (1992).

[6] R. Foot, O. F. Hernandez, F. Pisano, and V. Pleitez, Lepton masses in an $SU(3)_L \times U(1)_N$ gauge model, Phys. Rev. D **47**, 4158 (1993).

[7] P. H. Frampton, Chiral Dilepton Model and the Flavor Question, Phys. Rev. Lett. **69**, 2889 (1992).

[8] H. N. Long, $SU(3)_L \times U(1)_N$ model for right-handed neutrino neutral currents, Phys. Rev. D **54**, 4691 (1996).

[9] H. N. Long, The 331 model with right handed neutrinos, Phys. Rev. D **53**, 437 (1996).

[10] R. Foot, H. N. Long, and T. A. Tran, $SU(3)_L \otimes U(1)_N$ and $SU(4)_L \otimes U(1)_N$ gauge models with right-handed neutrinos, Phys. Rev. D **50**, R34 (1994).

[11] C. A. de Sousa Pires and O. P. Ravinez, Charge quantization in a chiral bilepton gauge model, Phys. Rev. D **58**, 035008 (1998).

[12] P. V. Dong and H. N. Long, Electric charge quantization in $SU(3)_C \times SU(3)_L \times U(1)_X$ models, Int. J. Mod. Phys. A **21**, 6677 (2006).

[13] J. C. Montero, V. Pleitez, and O. Ravinez, Soft superweak CP violation in a 331 model, Phys. Rev. D **60**, 076003 (1999).

[14] J. C. Montero, C. C. Nishi, V. Pleitez, O. Ravinez, and M. C. Rodriguez, Soft CP violation in K meson systems, Phys. Rev. D **73**, 016003 (2006).

[15] P. B. Pal, The strong CP question in $SU(3)_C \times SU(3)_L \times U(1)_N$ models, Phys. Rev. D **52**, 1659 (1995).

[16] A. G. Dias, V. Pleitez, and M. D. Tonasse, Naturally light invisible axion in models with large local discrete symmetries, Phys. Rev. D **67**, 095008 (2003).

[17] A. G. Dias and V. Pleitez, Stabilizing the invisible axion in 3-3-1 models, Phys. Rev. D **69**, 077702 (2004).

[18] A. G. Dias, C. A. de S. Pires, and P. S. Rodrigues da Silva, Discrete symmetries, invisible axion and lepton number symmetry in an economic 3-3-1 model, Phys. Rev. D **68**, 115009 (2003).

[19] A. E. Cárcamo Hernández, S. Kovalenko, H. N. Long, and I. Schmidt, A variant of 3-3-1 model for the generation of the SM fermion mass and mixing pattern, J. High Energy Phys. 07 (2018) 144.

[20] K. Huitu and N. Koivunen, Froggatt-Nielsen mechanism in a model with $SU(3)_c \times SU(3)_L \times U(1)_X$ gauge group, Phys. Rev. D **98**, 011701 (2018).

[21] D. Chang and H. N. Long, Interesting radiative patterns of neutrino mass in an $SU(3)_c \times SU(3)_L \times U(1)_X$ model with right-handed neutrinos, Phys. Rev. D **73**, 053006 (2006).

[22] C. Salazar, R. H. Benavides, W. A. Ponce, and E. Rojas, LHC constraints on 3-3-1 models, J. High Energy Phys. 07 (2015) 096.

[23] A. J. Buras, F. De Fazio, J. Girrbach, and M. V. Carlucci, The anatomy of quark flavour observables in 331 models in the flavour precision era, J. High Energy Phys. 02 (2013) 023.

[24] A. E. Cárcamo Hernández, R. Martinez, and F. Ochoa, Z and Z' decays with and without FCNC in 331 models, Phys. Rev. D **73**, 035007 (2006).

[25] R. Martinez and F. Ochoa, Mass-matrix ansatz and constraints on B0(s)—anti-B0(s) mixing in 331 models, Phys. Rev. D **77**, 065012 (2008).

[26] A. J. Buras, F. De Fazio, and J. Girrbach, 331 models facing new $b \to s\mu^+\mu^-$ data, J. High Energy Phys. 02 (2014) 112.

[27] A. J. Buras, F. De Fazio, and J. Girrbach-Noe, $Z - Z'$ mixing and Z-mediated FCNCs in $SU(3)_C \times SU(3)_L \times U(1)_X$ models, J. High Energy Phys. 08 (2014) 039.

[28] V. T. N. Huyen, H. N. Long, T. T. Lam, and V. Q. Phong, Neutral current in reduced minimal 3-3-1 model, Commun. Phys. **24**, 97 (2014).

[29] H. N. Long and T. Inami, S, T, U parameters in $SU(3)_C \times SU(3)_L \times U(1)_X$ model with right-handed neutrinos, Phys. Rev. D **61**, 075002 (2000).

[30] M. Tanabashi *et al.* (Particle Data Group), Review of particle physics, Phys. Rev. D **98**, 030001 (2018).

[31] P. V. Dong, H. N. Long, D. T. Nhung, and D. V. Soa, $SU(3)_C \times SU(3)_L \times U(1)_X$ model with two Higgs triplets, Phys. Rev. D **73**, 035004 (2006).

[32] F. S. Queiroz, C. Siqueira, and J. W. F. Valle, Constraining flavor changing interactions from LHC run-2 dilepton bounds with vector mediators, Phys. Lett. B **763**, 269 (2016).

[33] V. Q. Phong, N. T. Tuong, N. C. Thao, and H. N. Long, Multiperiod structure of electroweak phase transition in the 3-3-1-1 model, Phys. Rev. D **99**, 015035 (2019).

[34] M. J. Baker, M. Breitbach, J. Kopp, and L. Mittnacht, Dynamic freeze-in: Impact of thermal masses and cosmological phase transitions on dark matter production, J. High Energy Phys. 03 (2018) 114.

[35] D. López-Val and T. Robens, Δr and the W-boson mass in the singlet extension of the standard model, Phys. Rev. D **90**, 114018 (2014).

[36] A. E. Cárcamo Hernández, I. de Medeiros Varzielas, and E. Schumacher, Fermion and scalar phenomenology of a two-Higgs-doublet model with S_3, Phys. Rev. D **93**, 016003 (2016).

[37] D. Lopez-Val and J. Sola, Delta r in the two-Higgs-doublet model at full one loop level—and beyond, Eur. Phys. J. C **73**, 2393 (2013).

[38] M. Drees and K. Hagiwara, Supersymmetric contribution to the electroweak ρ parameter, Phys. Rev. D **42**, 1709 (1990).

[39] M. Aaboud *et al.* (ATLAS Collaboration), Search for additional heavy neutral Higgs and gauge bosons in the ditau final state produced in 36 fb^{-1} of pp collisions at $\sqrt{s} = 13$ TeV with the ATLAS detector, J. High Energy Phys. 01 (2018) 055.

[40] M. Aaboud *et al.* (ATLAS Collaboration), Search for charged Higgs bosons decaying via $H^\pm \to \tau^\pm \nu_\tau$ in the $\tau +$ jets and $\tau +$ lepton final states with 36 fb^{-1} of pp collision data recorded at $\sqrt{s} = 13$ TeV with the ATLAS experiment, J. High Energy Phys. 09 (2018) 139.

[41] M. Aaboud *et al.* (ATLAS Collaboration), Search for heavy resonances decaying to a photon and a hadronically decaying $Z/W/H$ boson in pp collisions at $\sqrt{s} = 13$ TeV with the ATLAS detector, Phys. Rev. D **98**, 032015 (2018).

[42] V. Khachatryan *et al.* (CMS Collaboration), Search for high-mass diphoton resonances in protonproton collisions at 13 TeV and combination with 8 TeV search, Phys. Lett. B **767**, 147 (2017).

[43] M. Aaboud *et al.* (ATLAS Collaboration), Search for new phenomena in high-mass diphoton final states using 37 fb^{-1} of proton–proton collisions collected at $\sqrt{s} = 13$ TeV with the ATLAS detector, Phys. Lett. B **775**, 105 (2017).

[44] F. Deppisch and J. W. F. Valle, Enhanced lepton flavor violation in the supersymmetric inverse seesaw model, Phys. Rev. D **72**, 036001 (2005).

[45] A. Ilakovac and A. Pilaftsis, Flavour-violating charged lepton decays in seesaw-type models, Nucl. Phys. **B437**, 491 (1995).

[46] M. Lindner, M. Platscher, and F. S. Queiroz, A call for new physics: The muon anomalous magnetic moment and lepton flavor violation, Phys. Rep. **731**, 1 (2018).

[47] M. A. Perez, G. Tavares-Velasco, and J. J. Toscano, Two-body Z' decays in the minimal 3-3-1 model, Phys. Rev. D **69**, 115004 (2004).

[48] G. C. Branco, P. M. Ferreira, L. Lavoura, M. N. Rebelo, M. Sher, and J. P. Silva, Theory and phenomenology of two-Higgs-doublet models, Phys. Rep. **516**, 1 (2012).

[49] J. Edsjo and P. Gondolo, Neutralino relic density including coannihilations, Phys. Rev. D **56**, 1879 (1997).

[50] S. Bhattacharya, P. Poulose, and P. Ghosh, Multipartite interacting scalar dark matter in the light of updated LUX data, J. Cosmol. Astropart. Phys. 04 (2017) 043.

[51] J. Elias-Miro, J. R. Espinosa, G. F. Giudice, H. M. Lee, and A. Strumia, Stabilization of the electroweak vacuum by a scalar threshold effect, J. High Energy Phys. 06 (2012) 031.

[52] K. Kannike, Vacuum stability of a general scalar potential of a few fields, Eur. Phys. J. C **76**, 324 (2016).

[53] G. Cynolter, E. Lendvai, and G. Pocsik, Note on unitarity constraints in a model for a singlet scalar dark matter candidate, Acta Phys. Pol. B **36**, 827 (2005).

[54] P. A. R. Ade *et al.* (Planck Collaboration), Planck 2015 results. XIII. Cosmological parameters, Astron. Astrophys. **594**, A13 (2016).